



Probing Axion-Like Particles and Neutral Triple Gauge Couplings at the CEPC

Related collaborators :

Chong-Xing Yue (岳崇兴)

Shuo Yang (杨硕)

Ji-Chong Yang (杨冀翀)

Han Wang (王晗); Hua-Ying Zhang (张华莹); Yue-Qi Wang (王悦琪); Qing Fu (付擎); Chun-Jing Pan (潘春静)

Yu-Chen Guo

(郭禹辰)

Liaoning Normal University

Lecture of CEPC New Physics Workshop 2024
@ZZU, Aug, 31, 2024



Where to next?

- **Evidences for physics beyond the Standard Model**

- Dark matter, Baryon asymmetry, Neutrino masses, Dark energy, ...
- Hierarchy/Naturalness/Fine tuning problem

- **We haven't found any new particles!**



Where to next?

- Build an even larger collider → go to high energy → discover new particles!
(No guaranteed discovery!)
- Do precision measurements → discover new physics indirectly!

How to look for new physics?

How do we interpret the measurement results?

Model-dependent

SUSY, 2HDM...

New particles

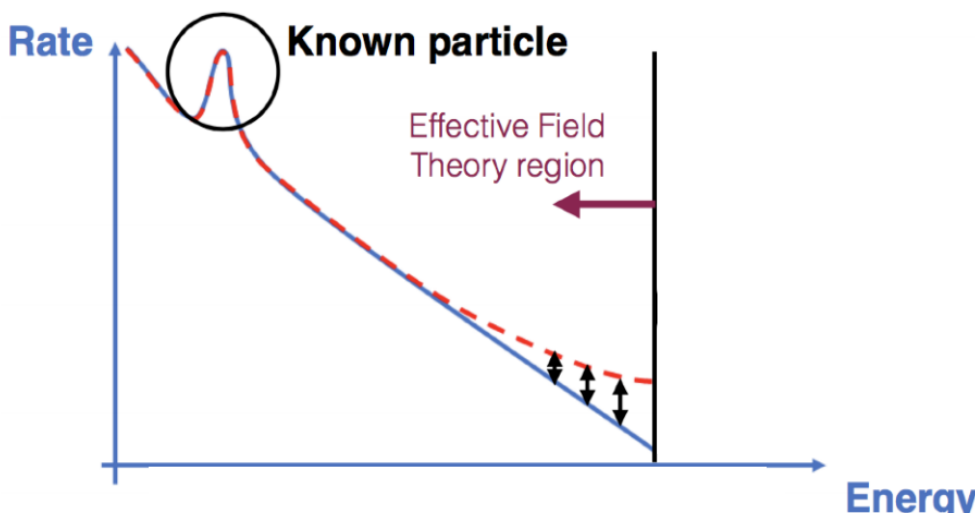
ALP, W', Z'...

Model-Independent

Simplified models, EFT

New Interactions
of SM particles

anomalous couplings



Deviations in tails

The first sign of new physics from precision measurements

Contents

I. Axion-Like Particles (ALPs) @ CEPC

- ALPs in light by light scattering (LBL)
- ALPs in tri-photon production
- ALPs in Z decay
- ALPs in vector boson fusion (VBF)

II. Anomalous Gauge Couplings

III. Summary

Properties of axion-like particles (ALPs)

- QCD axions: PecceiQuinn mechanism to solve “strong-CP”
- ALP: generalizations of QCD axions
- CP-odd neutral pseudoscalars
- Parameters: masses & couplings

Dimension-5
operators :

$$\begin{aligned} \mathcal{L}_{\text{eff}}^{D \leq 5} = & \frac{1}{2} (\partial_\mu a) (\partial^\mu a) - \frac{M_a^2}{2} a^2 + \frac{\partial^\mu a}{\Lambda} \sum_F \bar{\psi}_F C_F \gamma_\mu \psi_F \\ & + g_s^2 C_{GG} \frac{a}{\Lambda} G_{\mu\nu}^A \tilde{G}^{\mu\nu,A} + g^2 C_{WW} \frac{a}{\Lambda} W_{\mu\nu}^A \tilde{W}^{\mu\nu,A} + g'^2 C_{BB} \frac{a}{\Lambda} B_{\mu\nu} \tilde{B}^{\mu\nu} \end{aligned}$$

After electroweak symmetry breaking:

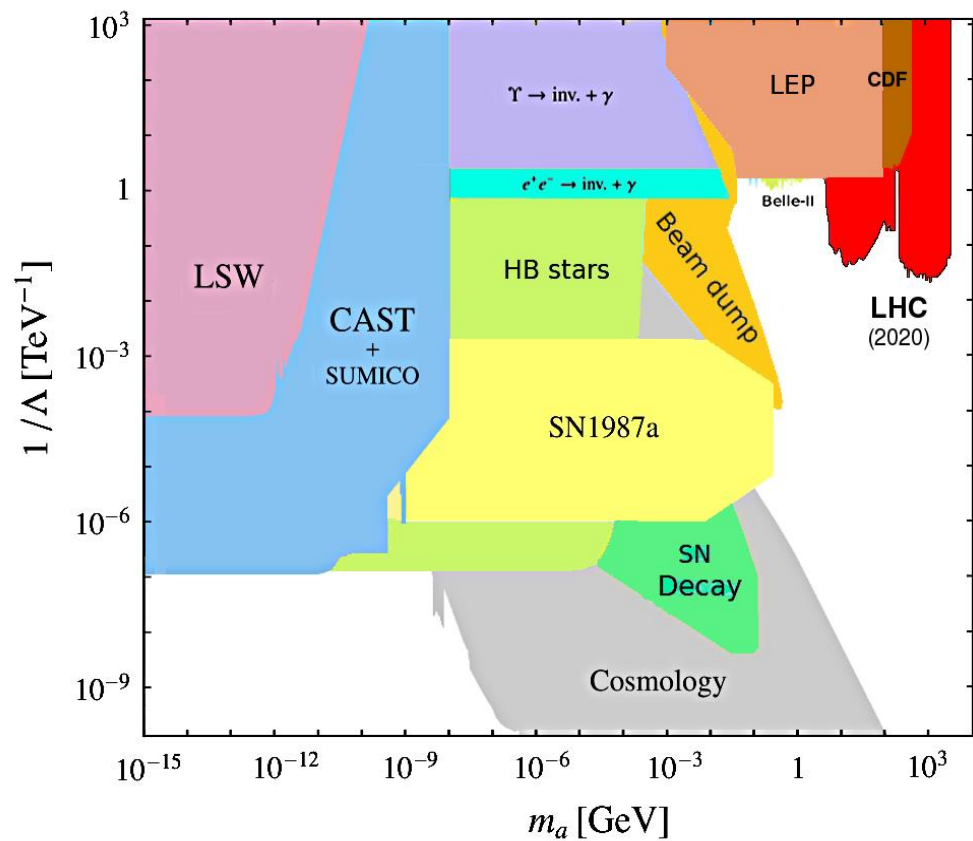
$$\begin{aligned} \mathcal{L}_{\text{eff}} = & \frac{1}{2} (\partial^\mu a) (\partial_\mu a) - \frac{1}{2} m_a^2 a^2 + i g_{a\psi} a \sum_{\psi=Q,L} m_\psi^{\text{diag}} \bar{\psi} \gamma_5 \psi \\ & - \frac{1}{4} g_{a\gamma\gamma} a F_{\mu\nu} \tilde{F}^{\mu\nu} - \frac{1}{4} g_{aZZ} a Z_{\mu\nu} \tilde{Z}^{\mu\nu} - \frac{1}{4} g_{a\gamma Z} a F_{\mu\nu} \tilde{Z}^{\mu\nu} \\ & - \frac{1}{4} g_{aWW} a W_{\mu\nu} \tilde{W}^{\mu\nu} \end{aligned}$$

with

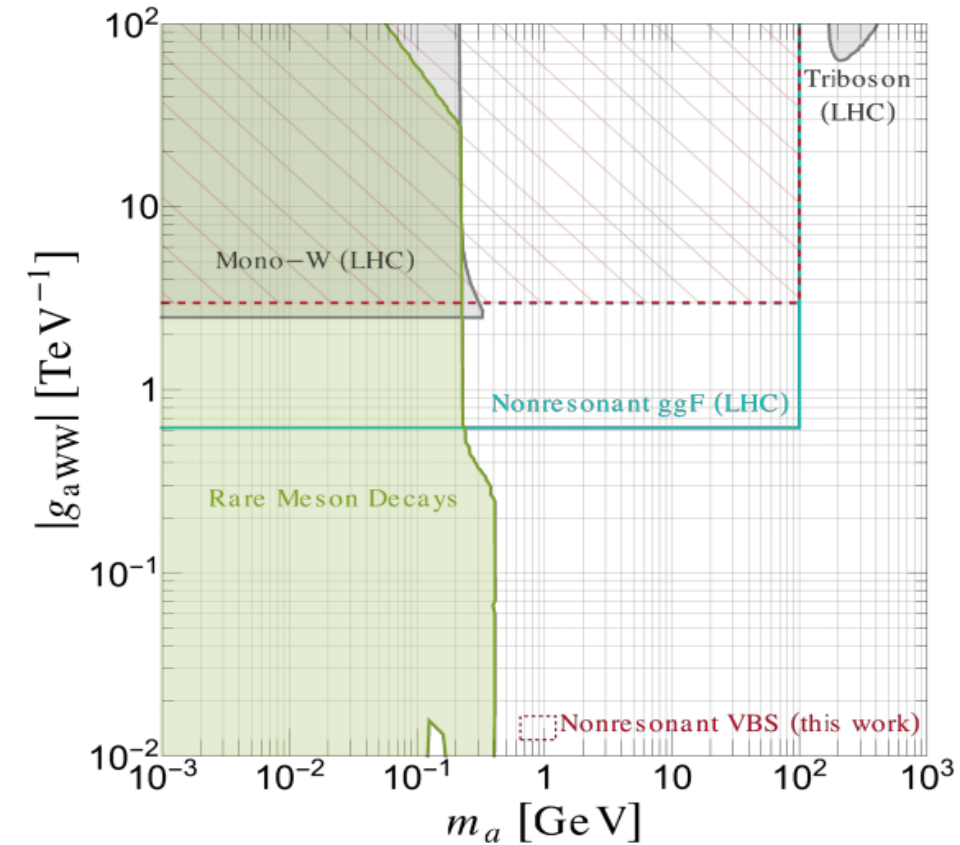
$$\begin{aligned} g_{a\gamma\gamma} &= \frac{4}{f_a} (c_W^2 C_{\tilde{B}} + s_W^2 C_{\tilde{W}}), & g_{aZZ} &= \frac{4}{f_a} (s_W^2 C_{\tilde{B}} + c_W^2 C_{\tilde{W}}), \\ g_{a\gamma Z} &= \frac{8}{f_a} s_W c_W (C_{\tilde{W}} - C_{\tilde{B}}), & g_{aWW} &= \frac{4}{f_a} C_{\tilde{W}} \end{aligned}$$

Constraints on the effective couplings of ALPs

D. Enterria (CERN), 2102.08971



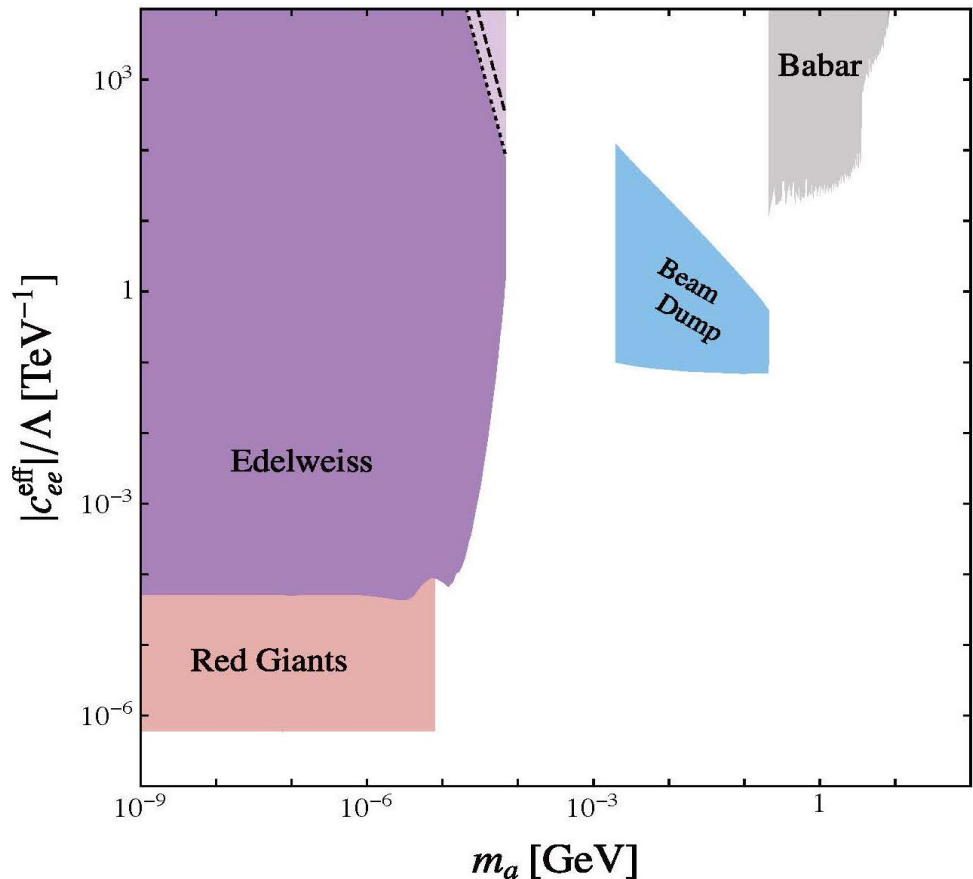
J. Bonilla et al., 2202.03450



Existing constraints on the ALP–photon coupling (left) and ALP–W coupling (right)

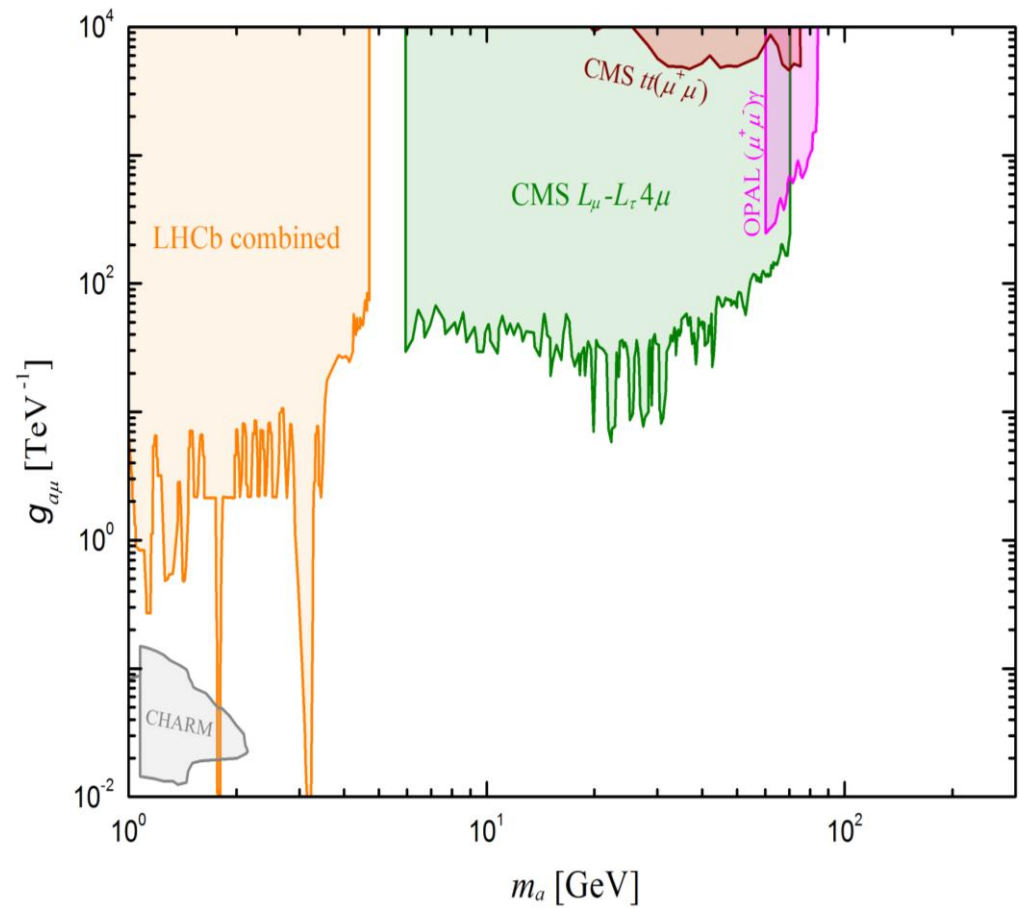
Constraints on the effective couplings of ALPs

M. Bauera, M. Neubert and A. Thamm, 1708.00443



B. Döbrich, et. al., 1810.11336

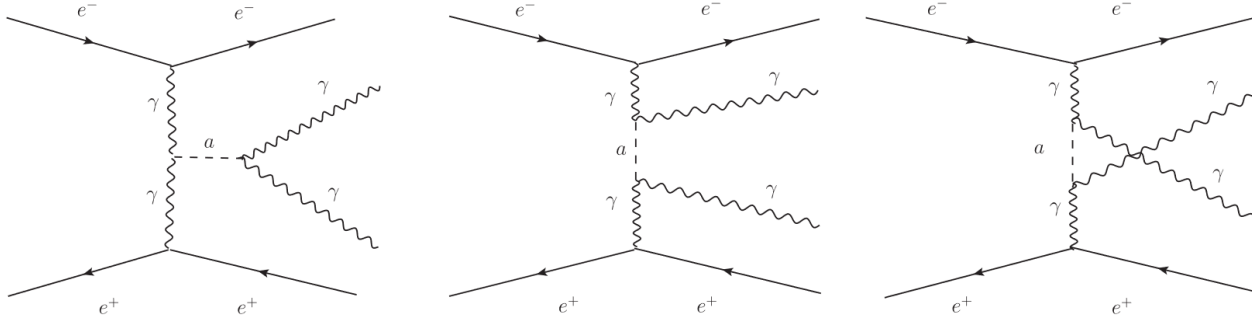
J. Liu, X.L. Ma, L.T. Wang, X.P. Wang, 2210.09335



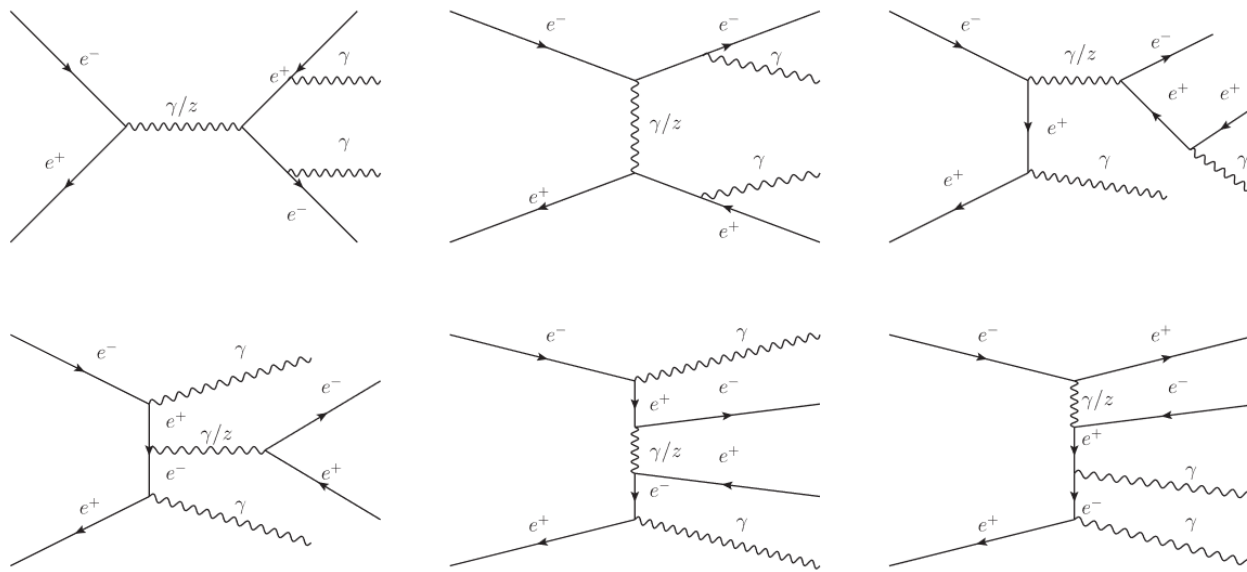
Existing constraints on the ALP–electron coupling (left) and ALP–muon coupling (right)

ALPs in Light by Light (LBL) Scattering

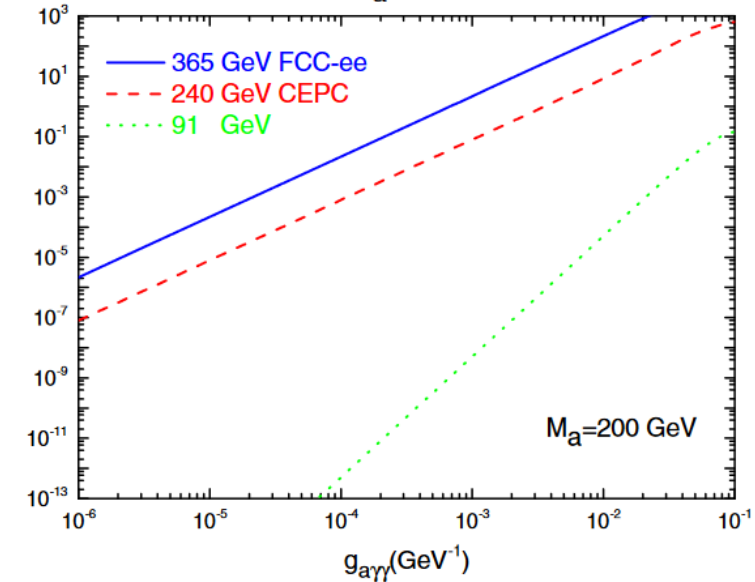
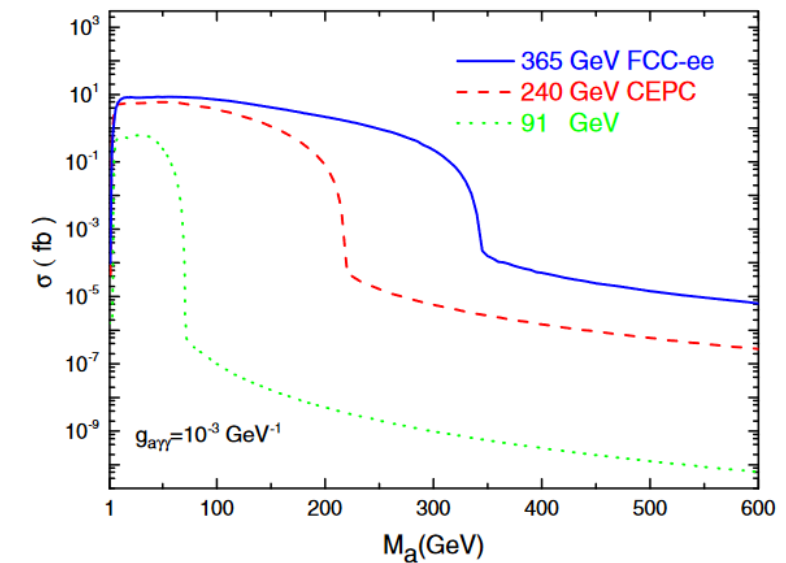
The Feynman diagrams of $e^+e^- \rightarrow a\gamma^* \rightarrow \gamma\gamma e^+e^-$



The typical diagrams for the background

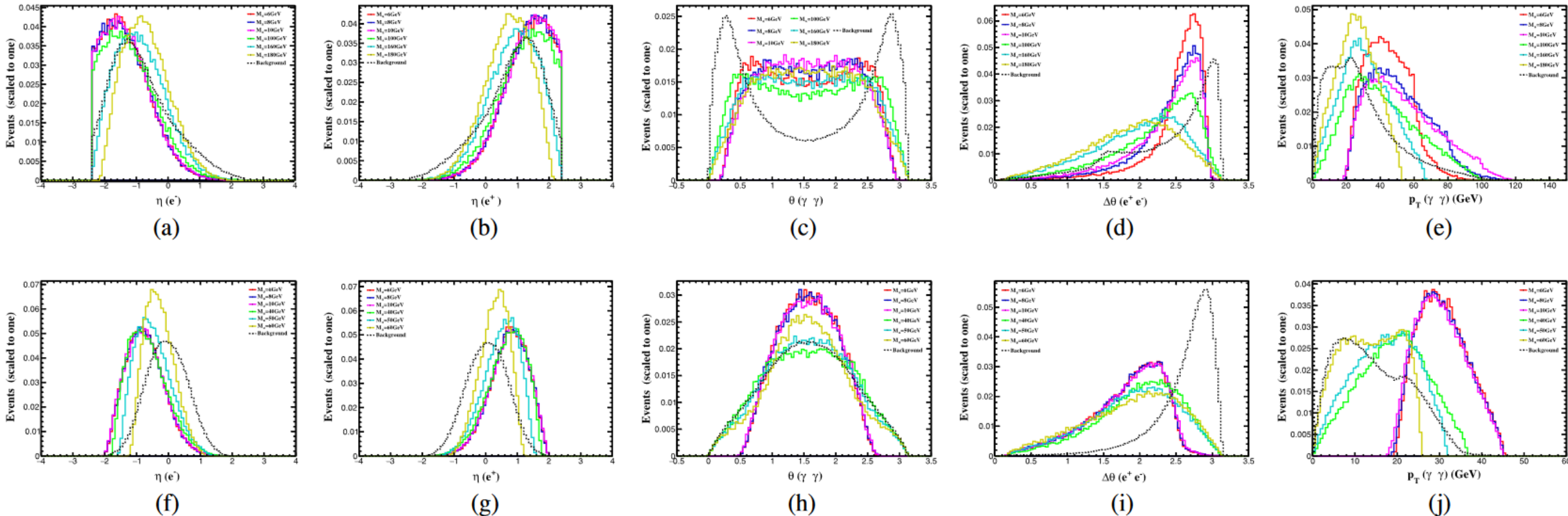


H.Y.Zhang, C.X.Yue, YCG, S.Yang, Phys. Rev. D (2021)



ALPs in Light by Light (LBL) Scattering

Normalized distributions of $\eta(e)$, $\theta(\gamma\gamma)$, $\theta(ee)$, $p_T(\gamma\gamma)$

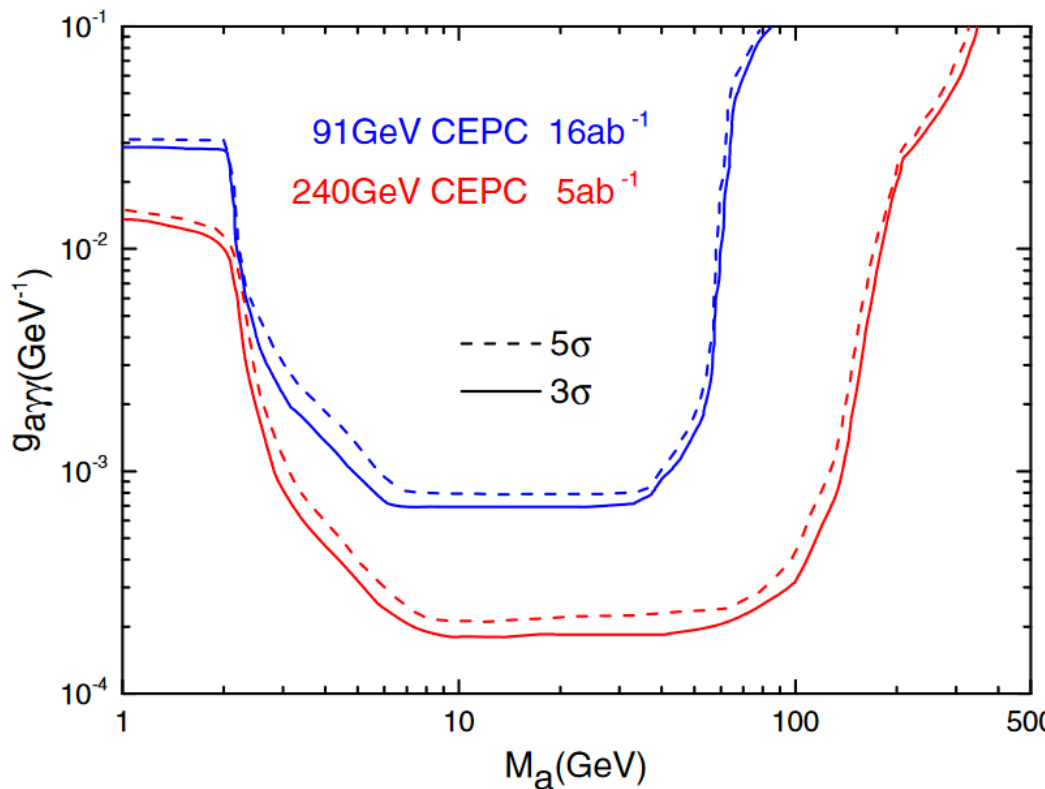


Cuts on
kinematic observables :

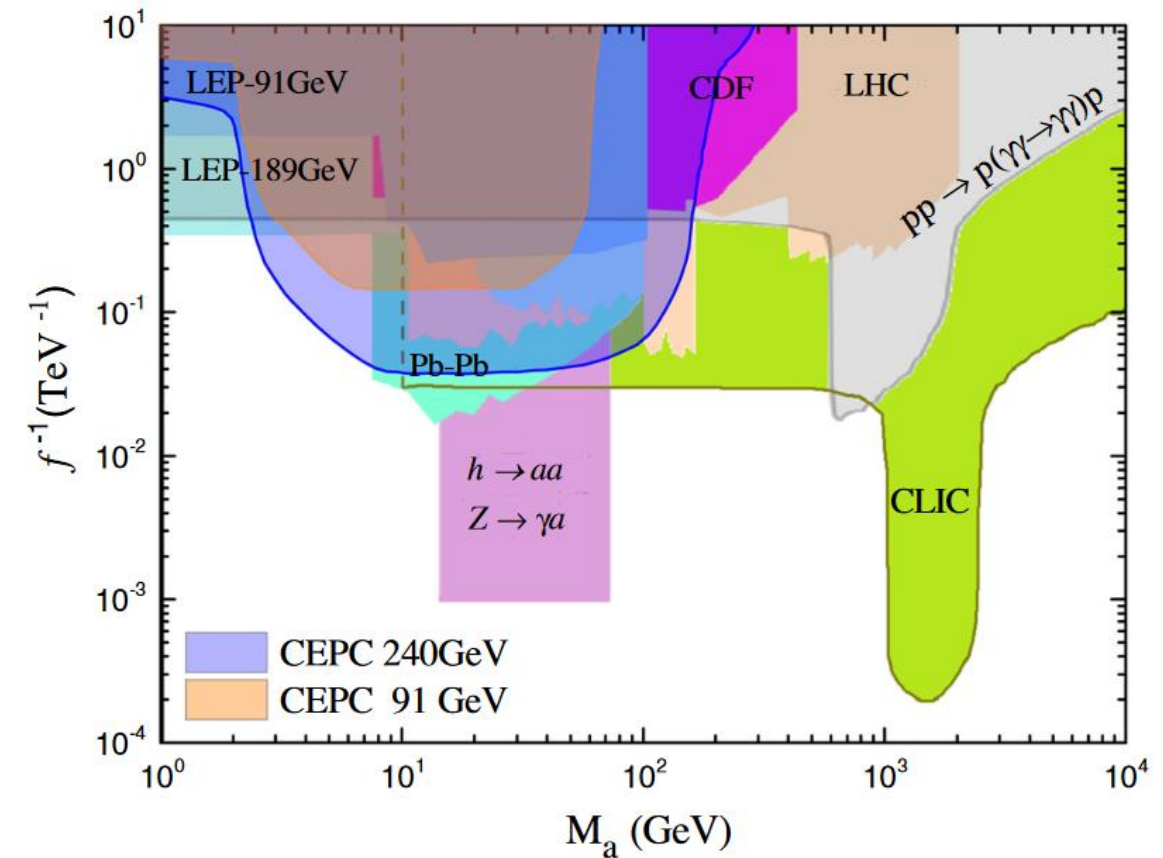
$$\begin{aligned} \sqrt{s} &= 240 \text{ GeV} \\ 0.4 &< \eta(e^+) < 2.4 \\ -2.4 &< \eta(e^-) < -0.4 \\ 0.7 &< \theta(\gamma\gamma) < 2.4 \\ \Delta\theta(e^+e^-) &< 2.9 \\ p_T(\gamma\gamma) &> 45 \text{ GeV} \end{aligned}$$

$$\begin{aligned} \sqrt{s} &= 91 \text{ GeV} \\ -0.3 &< \eta(e^+) < 0.9 \\ -0.9 &< \eta(e^-) < 0.3 \\ 0.7 &< \theta(\gamma\gamma) < 2.4 \\ \Delta\theta(e^+e^-) &< 2.4 \\ p_T(\gamma\gamma) &> 20 \text{ GeV} \end{aligned}$$

ALPs in Light by Light (LBL) Scattering



The sensitivities of the CEPC

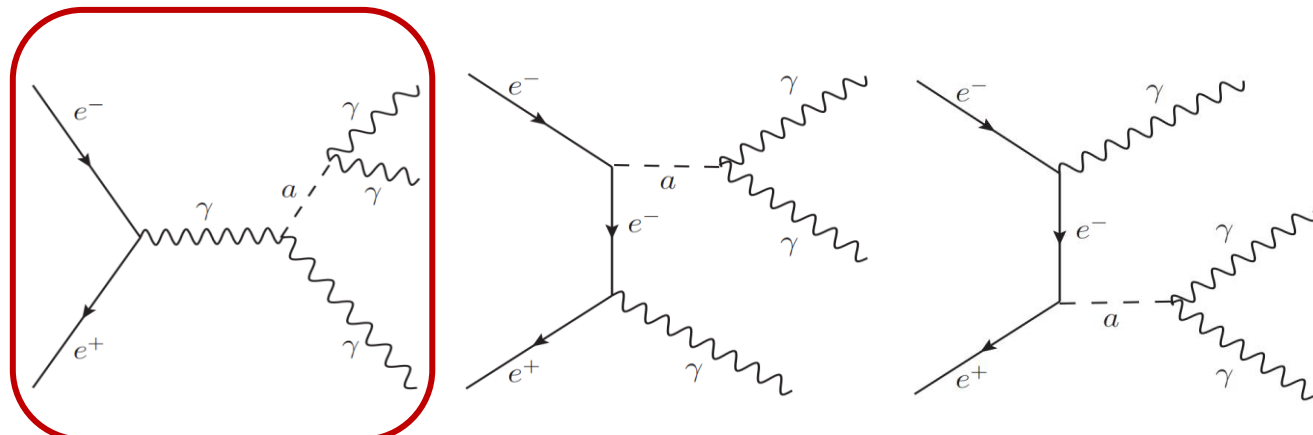


The 95% C.L. exclusion regions on the ALP couplings

ALPs in Tri-Photon Production

- The Feynman diagrams for the process of $e^+e^- \rightarrow a\gamma \rightarrow 3\gamma$

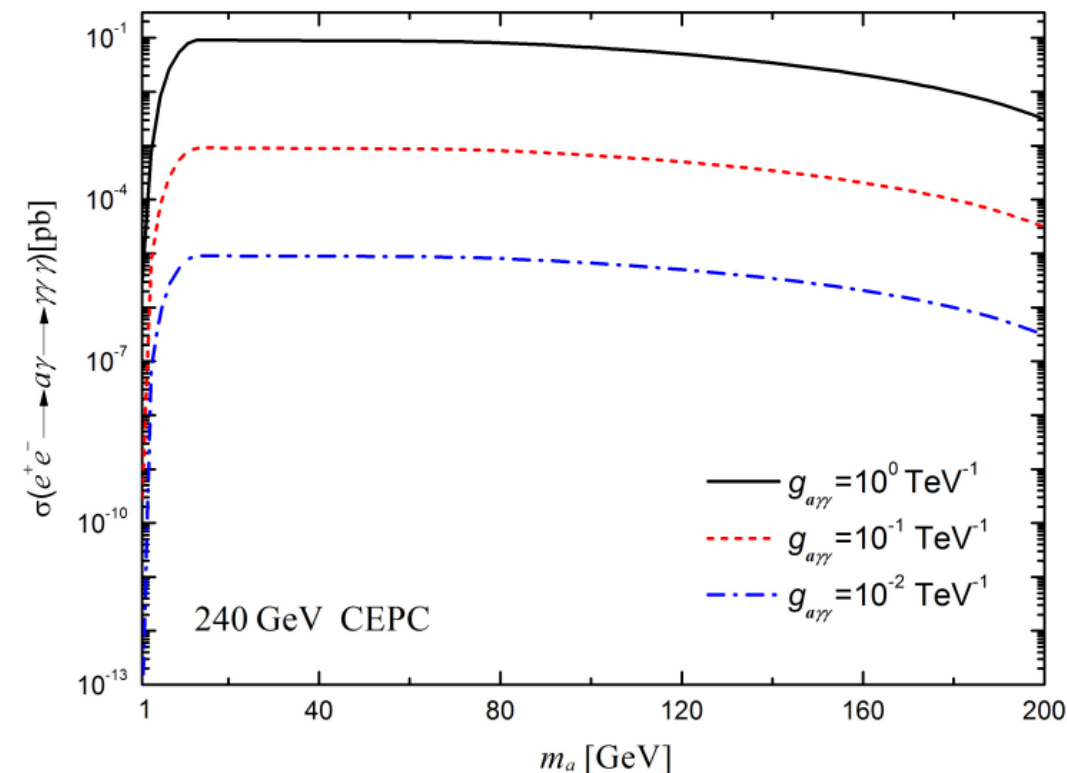
H.Wang, C.X.Yue, YCG, et.al. J. Phys. G (2022)



$$C_{\tilde{W}} = C_{\tilde{B}} \quad \rightarrow \quad g_{a\gamma\gamma} = g_{aZZ} = g_{aWW} \text{ and } g_{a\gamma Z} = 0$$

CEPC: $E_{CM} = 240 \text{ GeV}$ $\mathcal{L} = 5.6 \text{ ab}^{-1}$

$$1 \text{ GeV} < m_a \leq 200 \text{ GeV}$$



The cross section of the process $e^+e^- \rightarrow a\gamma \rightarrow 3\gamma$

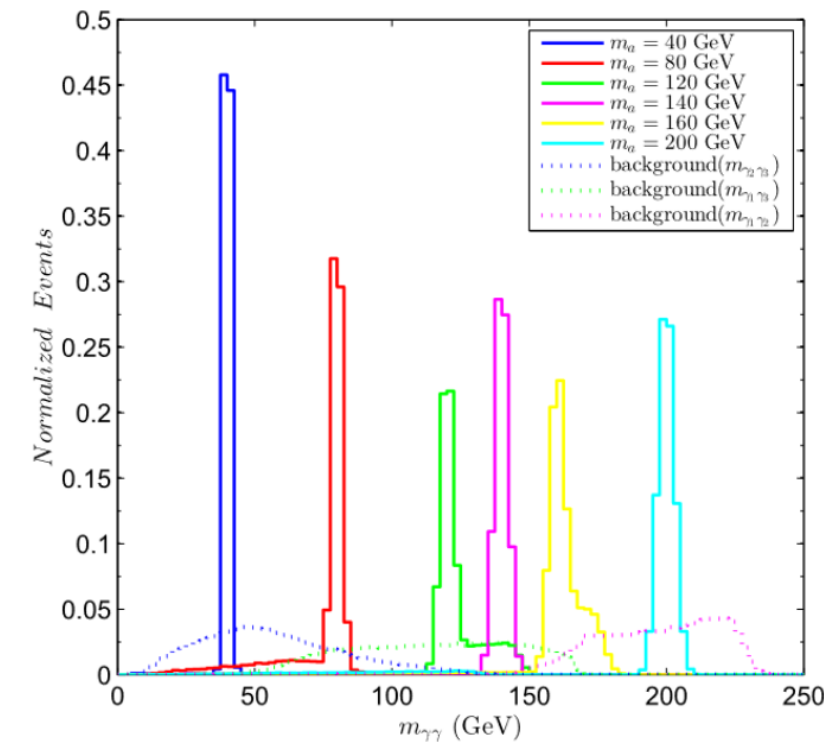
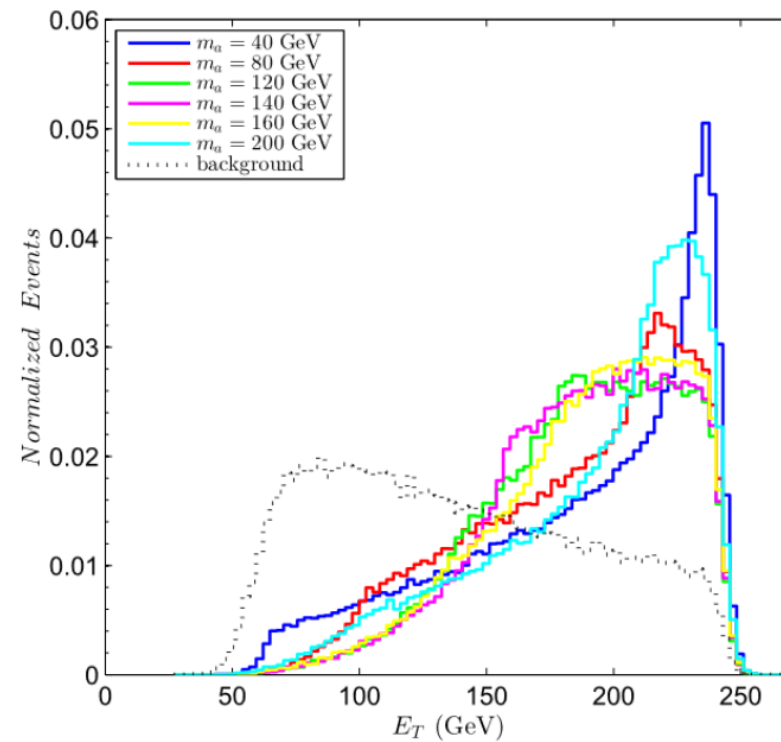
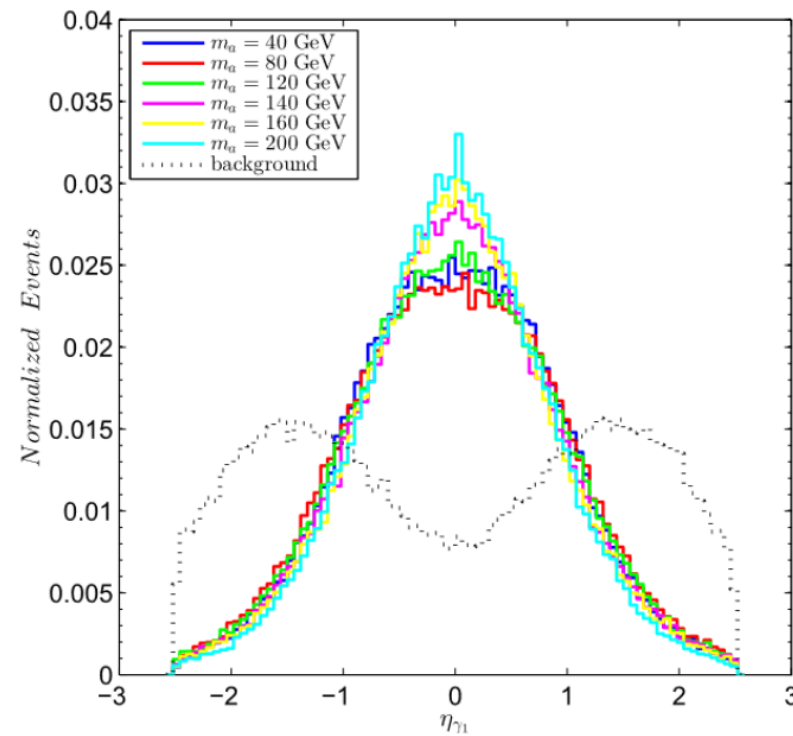
ALPs in Tri-Photon Production

Basic cuts: $p_T^\gamma > 10 \text{ GeV}$, $|\eta_\gamma| < 2.5$, $\Delta R_{\gamma\gamma} > 0.2$

$m_a \leq 20 \text{ GeV}$ $\longrightarrow N_\gamma \geq 1$

$m_a > 20 \text{ GeV}$ $\longrightarrow N_\gamma \geq 3$

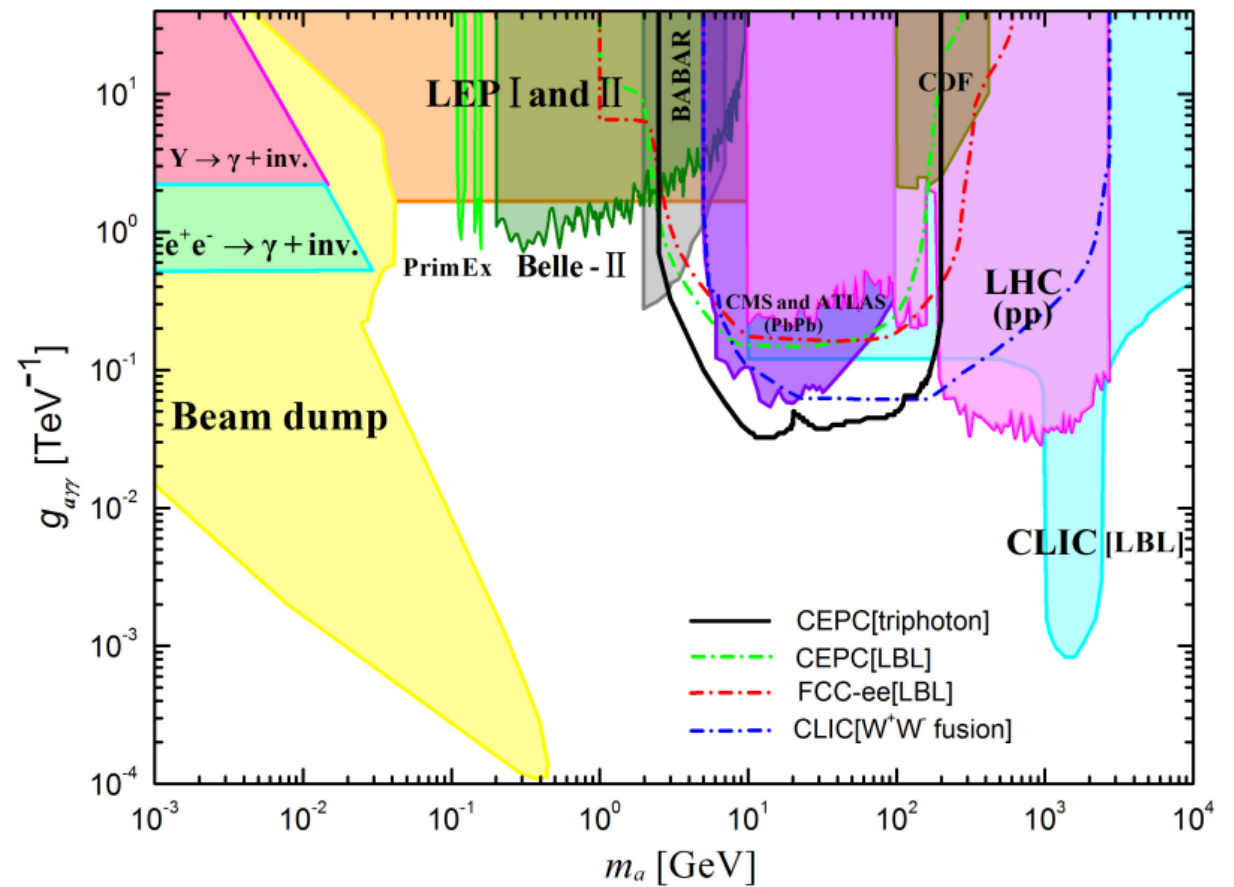
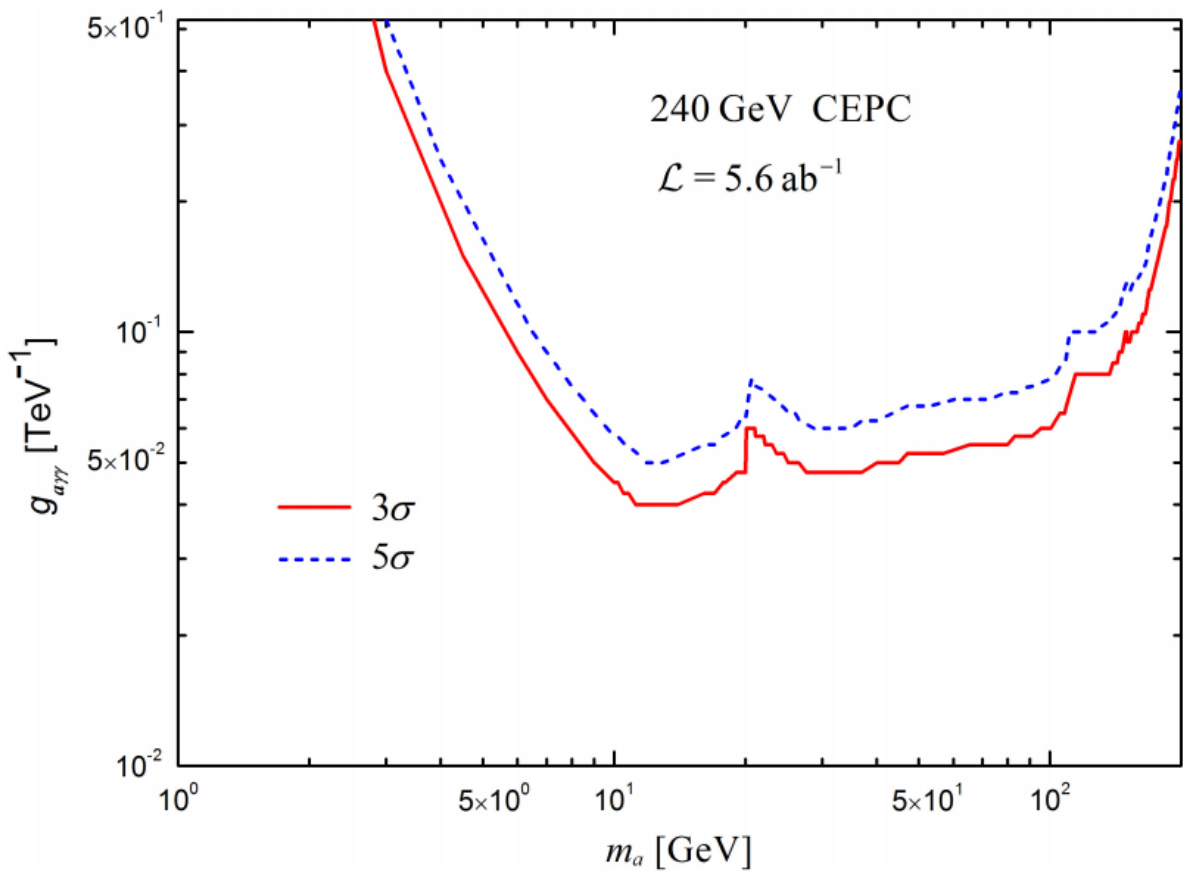
Normalized distributions of $\eta_{\gamma_1}, E_T, m_{\gamma\gamma}$



high mass ALP $\longrightarrow \gamma_1\gamma_2$

low mass ALP $\longrightarrow \gamma_2\gamma_3$

ALPs in Tri-Photon Production

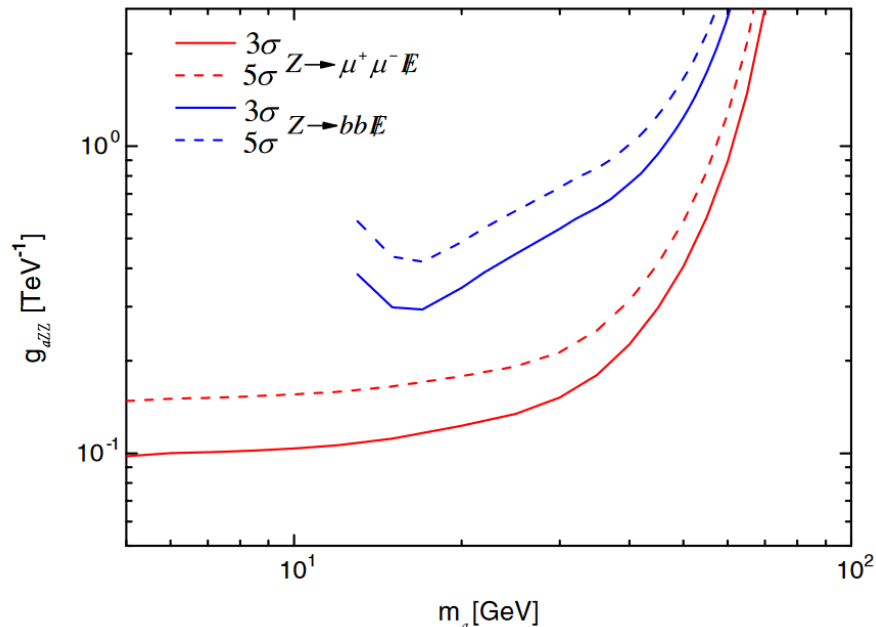
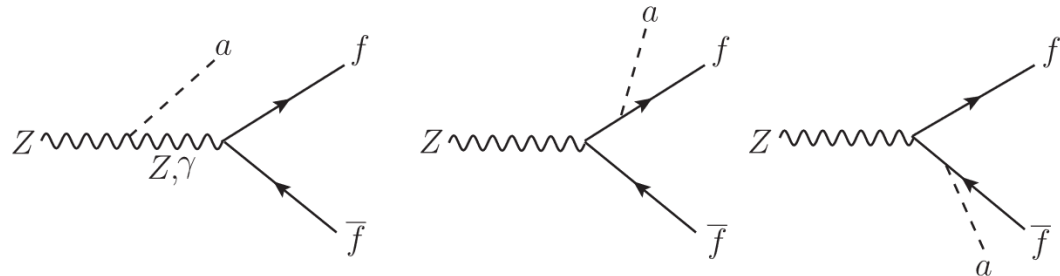


Left: The 3σ and 5σ curves for the process $e^+e^- \rightarrow a\gamma \rightarrow 3\gamma$ in the m_a - $g_{a\gamma\gamma}$ plane

Right: The promising sensitivities as $g_{a\gamma\gamma} \in [0.0325, 0.37]\text{GeV}^{-1}$ with $m_a \in [2.9, 190]\text{ GeV}$ at 2σ level

ALPs in the decay $Z \rightarrow a f \bar{f}$

The Feynman diagrams for exotic Z decay $Z \rightarrow a f \bar{f}$



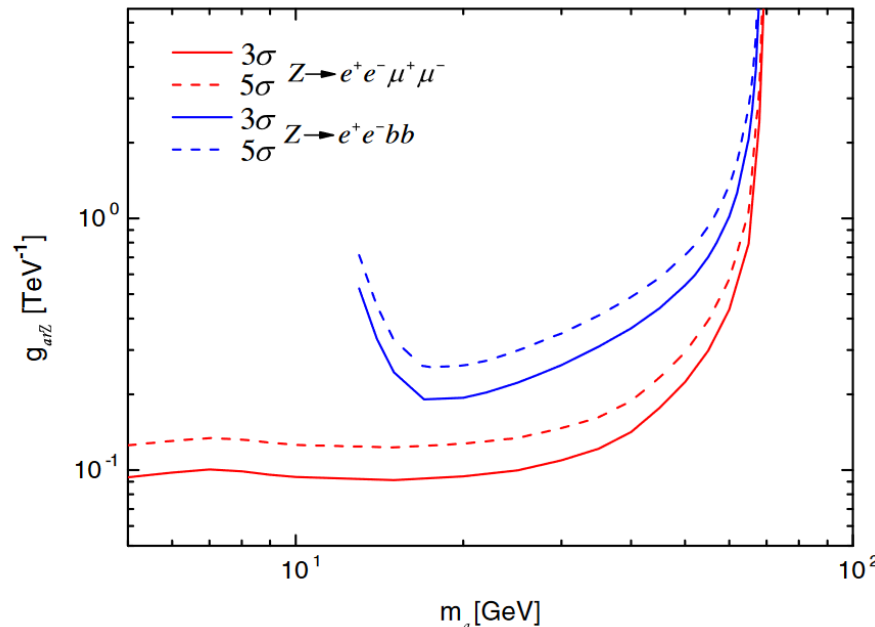
C.X.Yue, S.Yang, H.Wang, Phys. Rev. D (2022)

A. $Z \rightarrow \mu^+\mu^-E$

C. $Z \rightarrow e^+e^-\mu^+\mu^-$

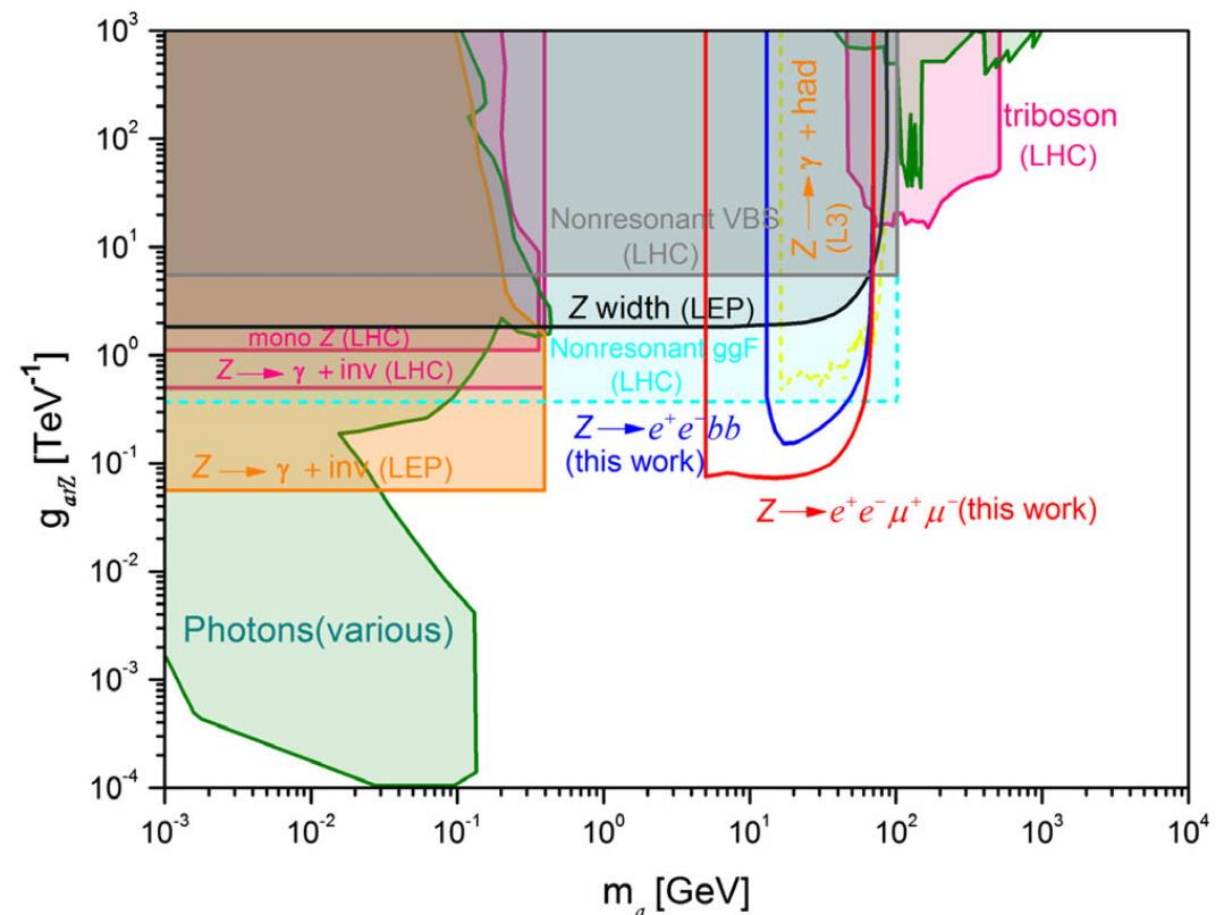
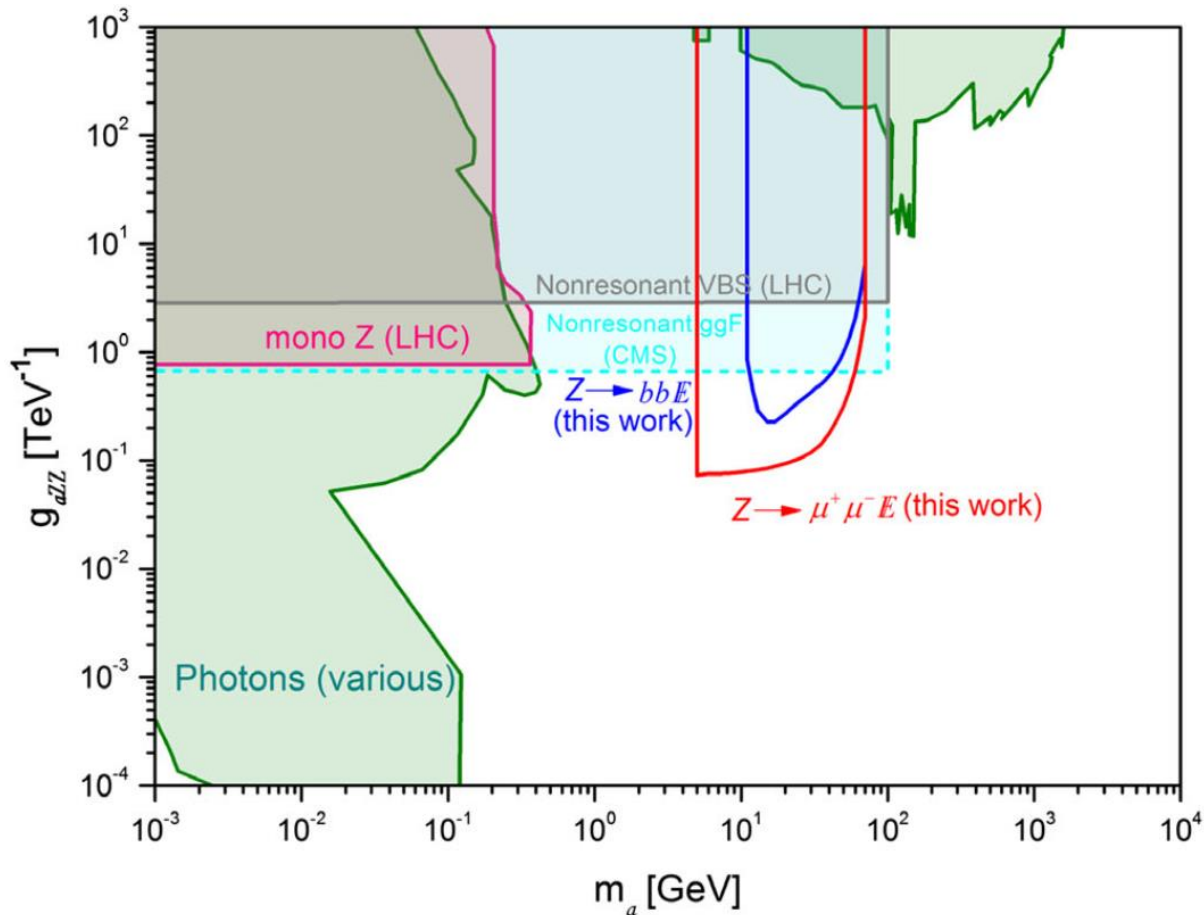
B. $Z \rightarrow bb\bar{E}$

D. $Z \rightarrow e^+e^-bb$



3 σ and 5 σ discovery curves for the Z factory with 1ab^{-1} integrated luminosity in the planes m_a - $g_{aZZ}(g_{aY\bar{Z}})$

ALPs in the decay $Z \rightarrow a f \bar{f}$

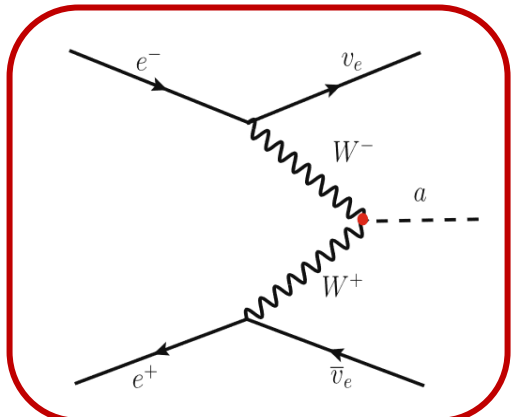


Sensitivity bounds on g_{aZZ} (left) and g_{ayZ} (right) at 95% C.L. from exotic Z decays and other current exclusion regions.

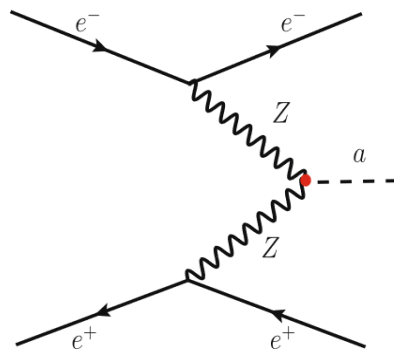
ALPs in Vector Boson Fusion (VBF)

- The Feynman diagrams for the process of $e^+e^- \rightarrow \nu\bar{\nu}a(\rightarrow \gamma\gamma)$

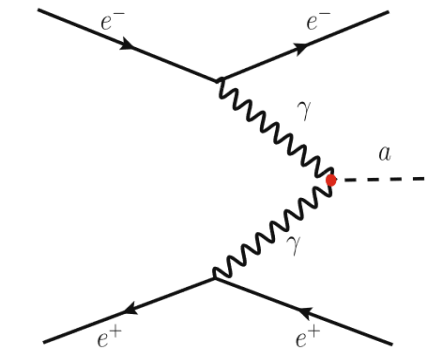
C.X.Yue, H.Y.Zhang, H.Wang, Eur. Phys. J. C(2022)



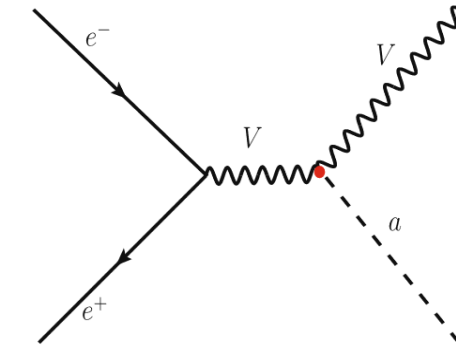
(a)



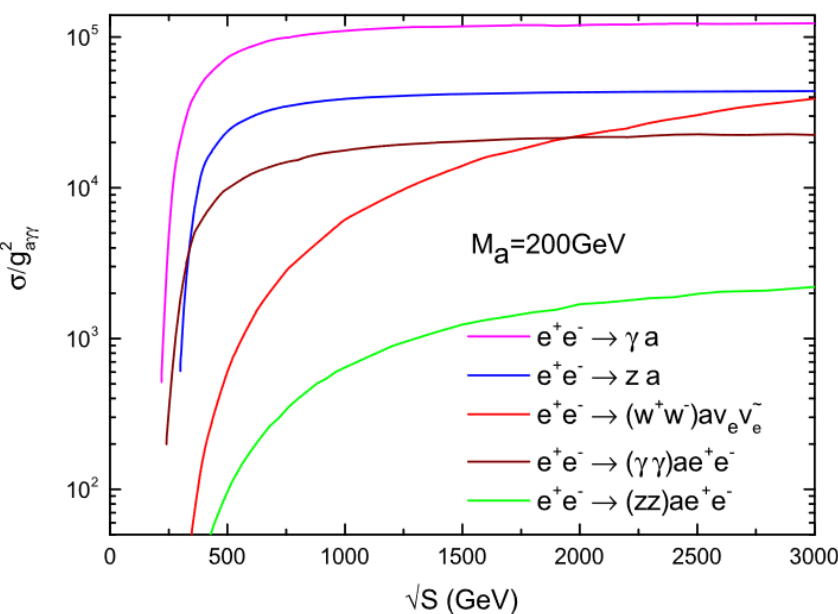
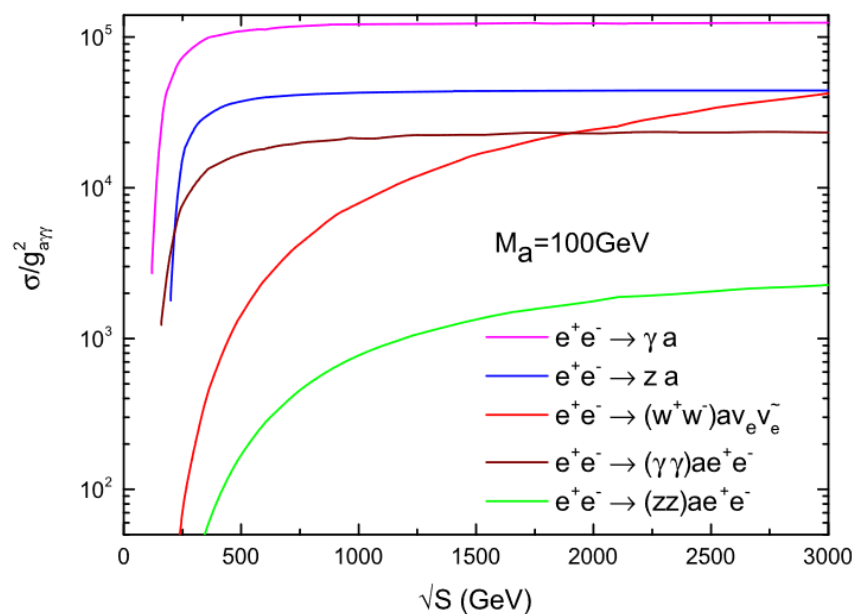
(b)



(c)



(d)

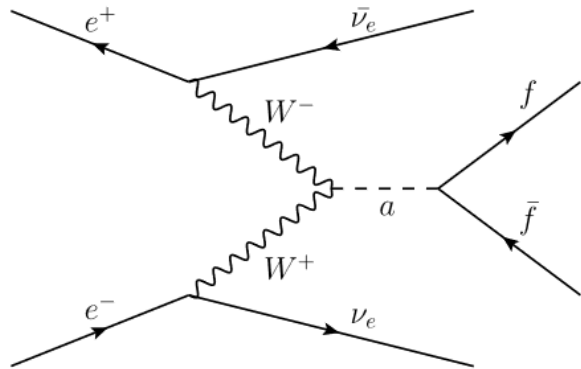


(c): S.C. Inan et. al. , 2003.01978
 S.C. Inan et. al. , 2007.01693
 H.-Y. Zhang et. al. , 2103.05218

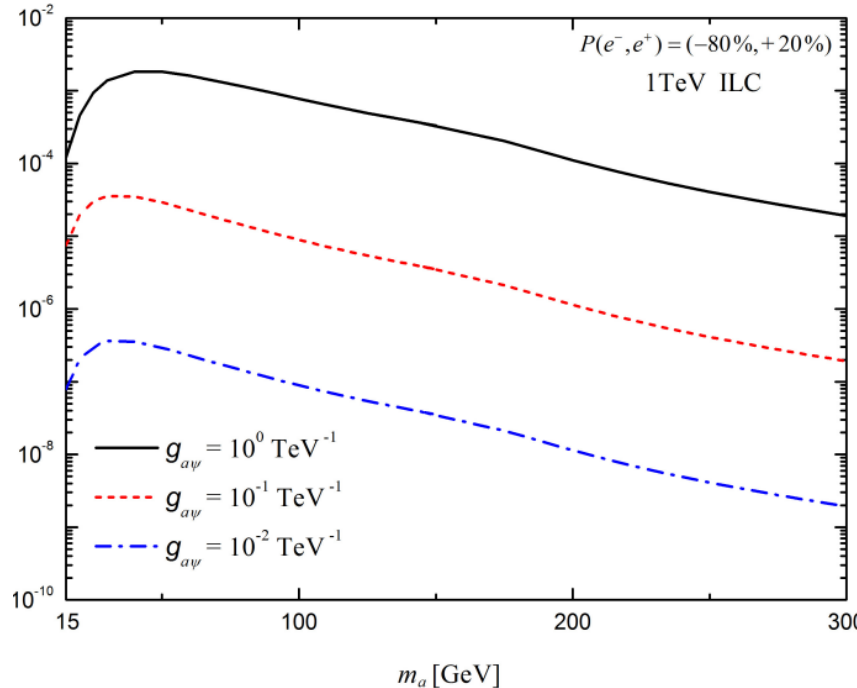
(d): M. Bauer et. al. , 1808.10323

ALPs in Vector Boson Fusion (VBF)

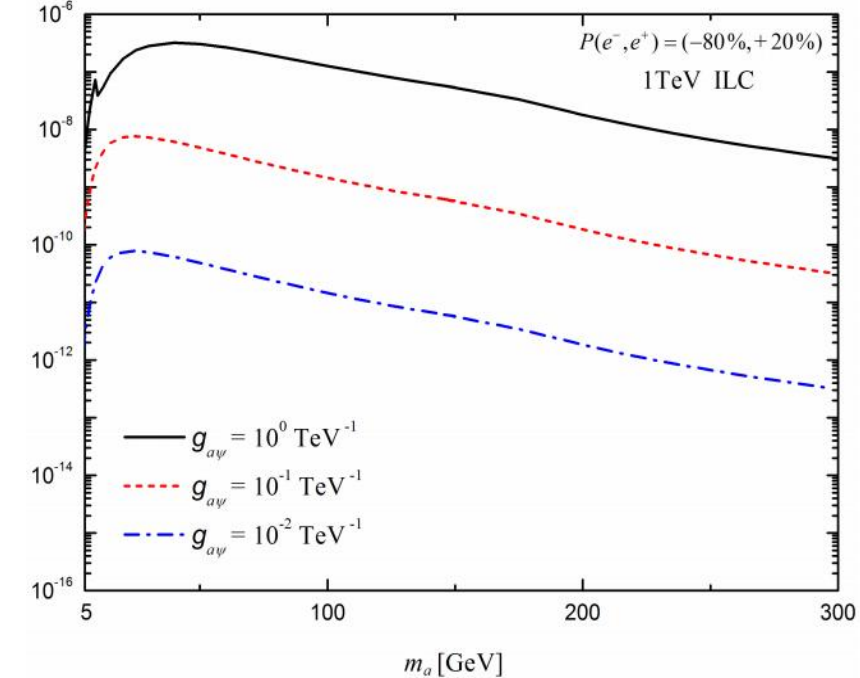
The Feynman diagrams for the process of $e^+e^- \rightarrow v\bar{v}a(\rightarrow f\bar{f})$



$$e^-e^+ \rightarrow v_e \bar{v}_e a (a \rightarrow b\bar{b})$$

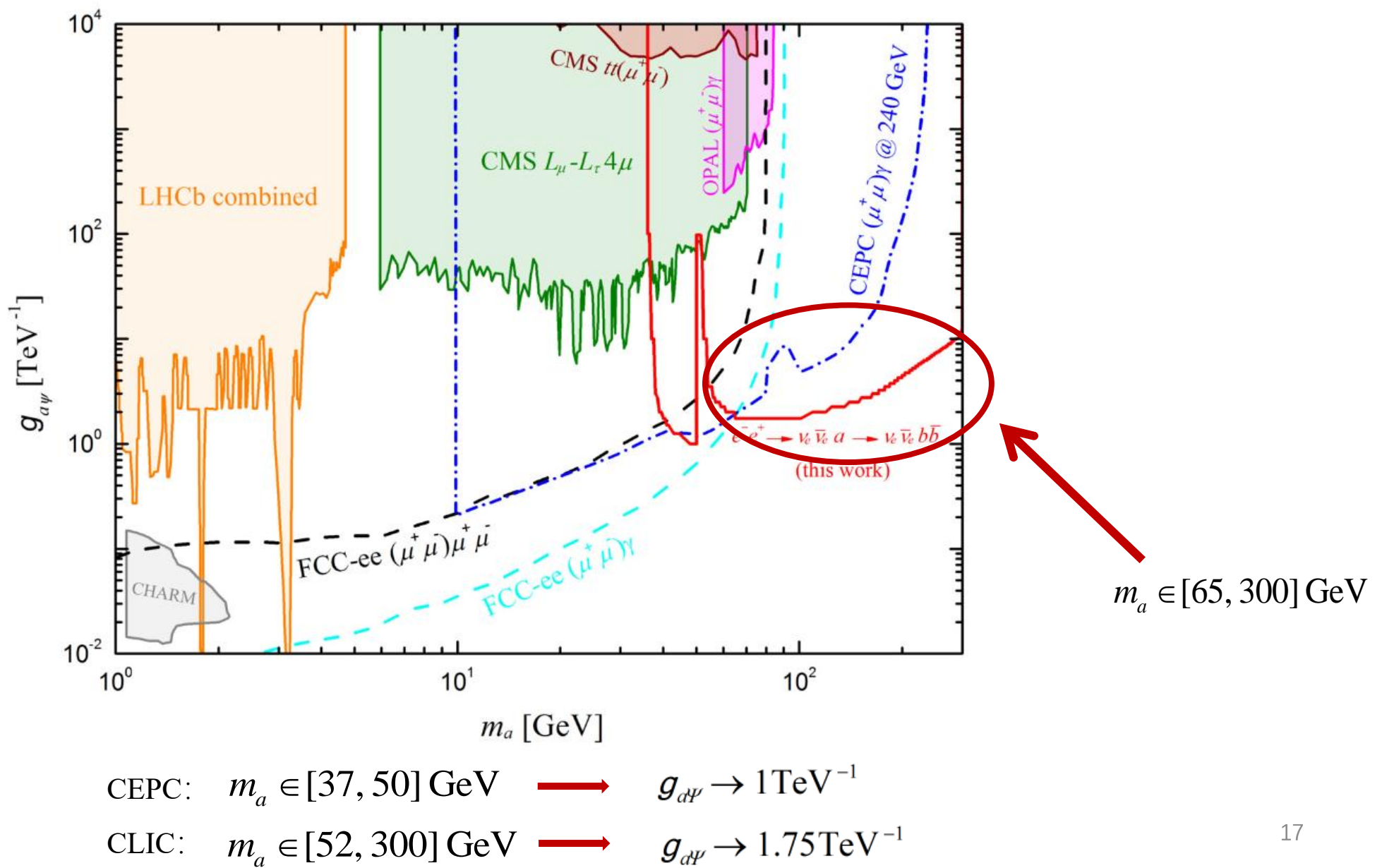


$$e^-e^+ \rightarrow v_e \bar{v}_e a (a \rightarrow \mu^+\mu^-)$$



The production cross sections of the $W+W-$ fusion processes for two decay channel

ALPs in Vector Boson Fusion (VBF)



Contents

- I. axion-like particles (ALPs)
- II. Neutral Triple Gauge Couplings (nTGCs)
 - nTGC in $Z\gamma$ production
 - nTGC in ZZ production
- III. Summary

Dimension-8 Operators affecting nTGC

$$\mathcal{L}_{\text{SMEFT}} = \mathcal{L}_{SM} + \sum_i \frac{C_{6i}}{\Lambda^2} \mathcal{O}_{6i} + \sum_j \frac{C_{8j}}{\Lambda^4} \mathcal{O}_{8j} + \dots$$

$$\mathcal{L}_{aQGC} = \sum_{i=0}^2 \frac{f_{S_i}}{\Lambda^4} O_{S_i} + \sum_{j=0}^7 \frac{f_{M_j}}{\Lambda^4} O_{M_j} + \sum_{k=0}^9 \frac{f_{T_k}}{\Lambda^4} O_{T_k}$$

$$\mathcal{L}_{\text{nTGC}} = \frac{\text{sign}(c_{\tilde{B}W})}{\Lambda_{\tilde{B}W}^4} \mathcal{O}_{\tilde{B}W} + \frac{\text{sign}(c_{B\tilde{W}})}{\Lambda_{B\tilde{W}}^4} \mathcal{O}_{B\tilde{W}} + \frac{\text{sign}(c_{\tilde{W}W})}{\Lambda_{\tilde{W}W}^4} \mathcal{O}_{\tilde{W}W} + \frac{\text{sign}(c_{\tilde{B}B})}{\Lambda_{\tilde{B}B}^4} \mathcal{O}_{\tilde{B}B},$$

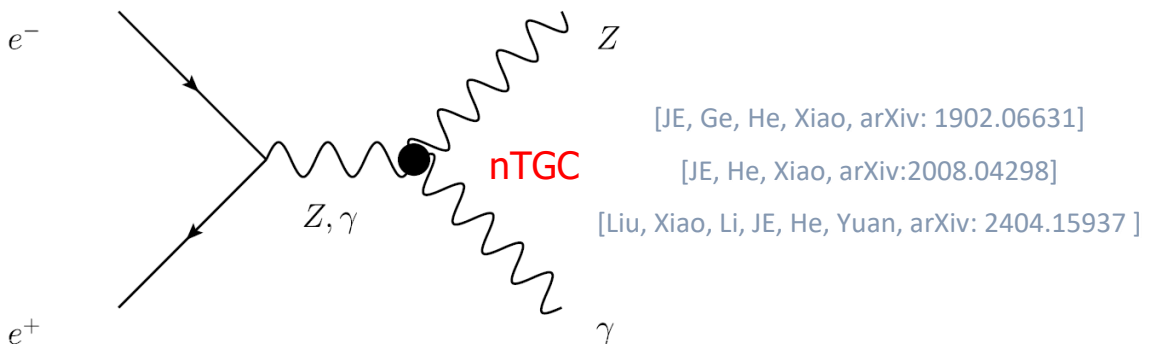
$$\begin{aligned}\mathcal{O}_{\tilde{B}W} &= iH^\dagger \tilde{B}_{\mu\nu} W^{\mu\rho} \{D_\rho, D^\nu\} H + h.c., \\ \mathcal{O}_{B\tilde{W}} &= iH^\dagger B_{\mu\nu} \tilde{W}^{\mu\rho} \{D_\rho, D^\nu\} H + h.c., \\ \mathcal{O}_{\tilde{W}W} &= iH^\dagger \tilde{W}_{\mu\nu} W^{\mu\rho} \{D_\rho, D^\nu\} H + h.c., \\ \mathcal{O}_{\tilde{B}B} &= iH^\dagger \tilde{B}_{\mu\nu} B^{\mu\rho} \{D_\rho, D^\nu\} H + h.c.,\end{aligned}$$

[C. Degrande, J. High Energy Phys. 02 (2014) 101]

The nTGCs provide a unique window to the BSM because they can arise from SMEFT operators only at the level of dim-8 or higher.

Diboson productions (ZA)

- nTGC in the $e^+ e^- \rightarrow Z\gamma$ process



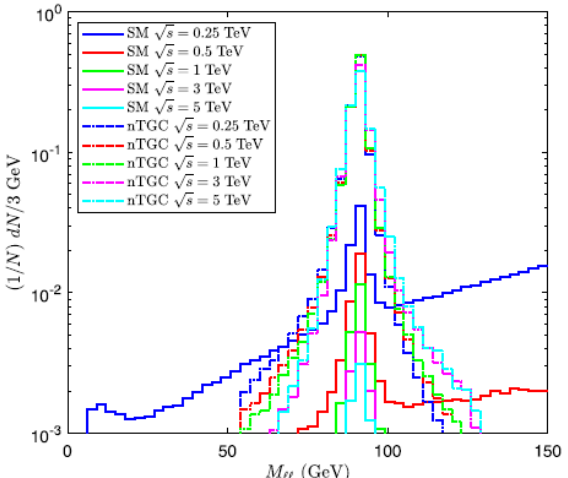
The constraints on $\text{sign}(c_{\tilde{B}W})/\Lambda_{\tilde{B}W}^4$ (TeV $^{-4}$) at $\mathcal{L} = 2 \text{ ab}^{-1}$ for leptonic decays.

S_{stat}	\sqrt{s} (GeV)				
	250	500	1000	3000	5000
2	[-25.7, 85.4]	[-5.2, 8.7]	[-1.0, 1.2]	[-0.12, 0.12]	[-0.054, 0.056]
3	[-34.9, 94.6]	[-6.7, 10.2]	[-1.3, 1.5]	[-0.15, 0.15]	[-0.067, 0.069]
5	[-50.1, 109.8]	[-9.0, 12.5]	[-1.7, 1.9]	[-0.19, 0.19]	[-0.088, 0.090]

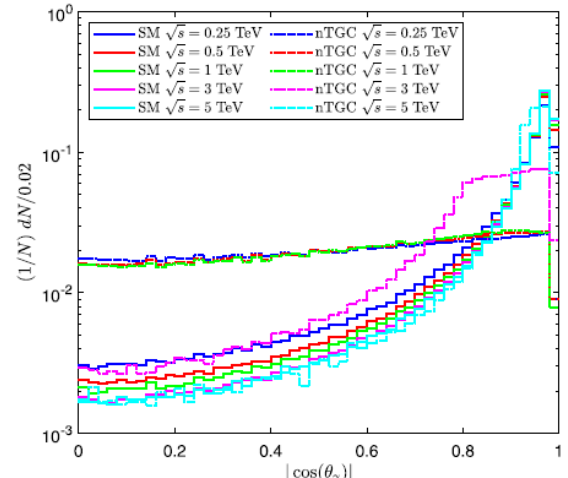
The expected constraints on $\text{sign}(c_{\tilde{B}W})/\Lambda_{\tilde{B}W}^4$ (TeV $^{-4}$) at $\mathcal{L} = 2 \text{ ab}^{-1}$ for hadronic Z decays.

S_{stat}	\sqrt{s} (GeV)				
	250 G	500	1000	3000	5000
2	[-10.5, 76.9]	[-1.0, 14.8]	[-0.35, 1.3]	[-0.030, 0.064]	[-0.013, 0.013]
3	[-14.9, 81.3]	[-1.5, 15.2]	[-0.48, 1.4]	[-0.040, 0.074]	[-0.016, 0.016]
5	[-22.7, 89.1]	[-2.3, 16.1]	[-0.69, 1.6]	[-0.055, 0.089]	[-0.020, 0.020]

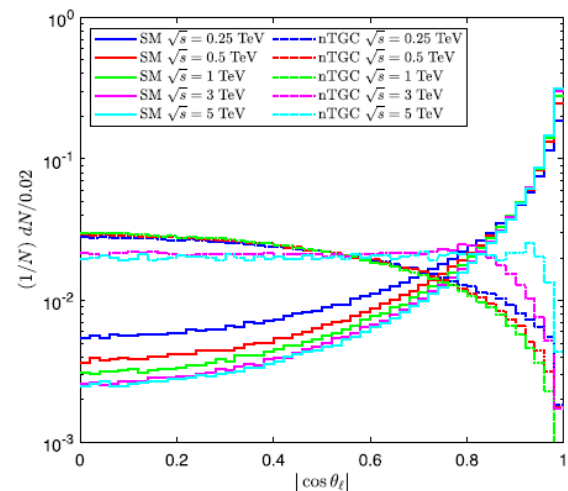
Q. Fu, J.-C. Yang, C.-X. Yue, Y-C. Guo, Nucl. Phys. B 972 (2021) 115543



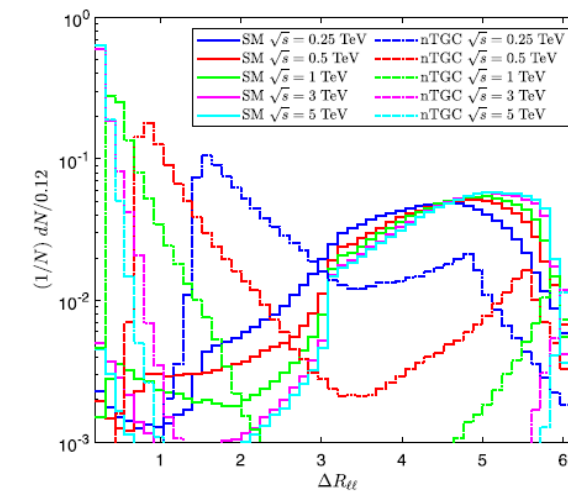
(a)



(b)



(c)



(d)

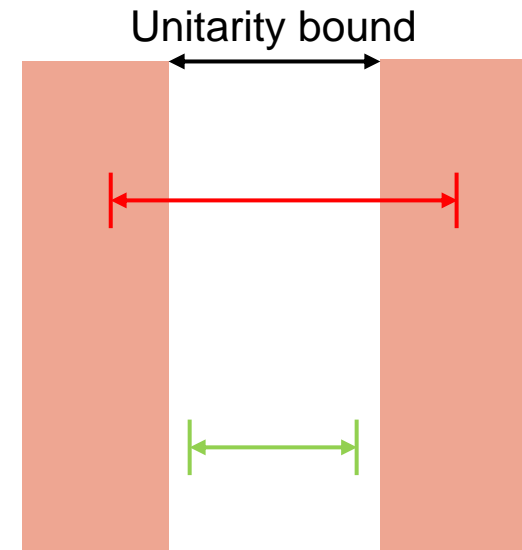
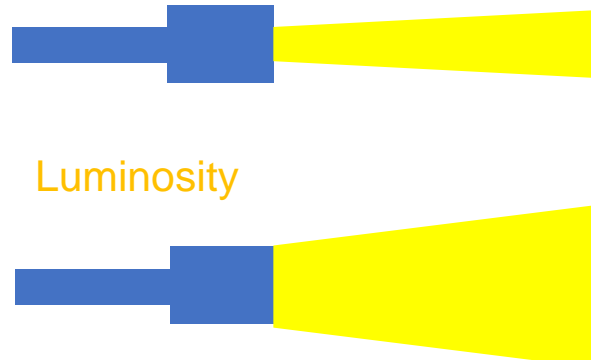
Diboson productions (ZA)

Unitary bounds can constrain operators directly for diboson production

$$\Lambda_{\tilde{B}W}^{+-,0+} \geq \left(\frac{e^2 \sqrt{s} v^2 (s - M_Z^2)}{48\sqrt{2}\pi M_Z c_W^2} \right)^{\frac{1}{4}}, \quad \Lambda_{\tilde{B}W}^{+-,++} \geq \left(\frac{e^2 v^2 (s - M_Z^2)}{48\sqrt{2}\pi c_W^2} \right)^{\frac{1}{4}},$$

$$\Lambda_{\tilde{B}W}^{-+,0+} \geq \left(\frac{e^2 \sqrt{s} (1 - 2s_W^2) v^2 (s - M_Z^2)}{96\sqrt{2}\pi M_Z s_W^2 c_W^2} \right)^{\frac{1}{4}},$$

$$\Lambda_{\tilde{B}W}^{-+,++} \geq \left(\frac{e^2 (2s_W^2 - 1) v^2 (M_Z^2 - s)}{96\sqrt{2}\pi s_W^2 c_W^2} \right)^{\frac{1}{4}},$$



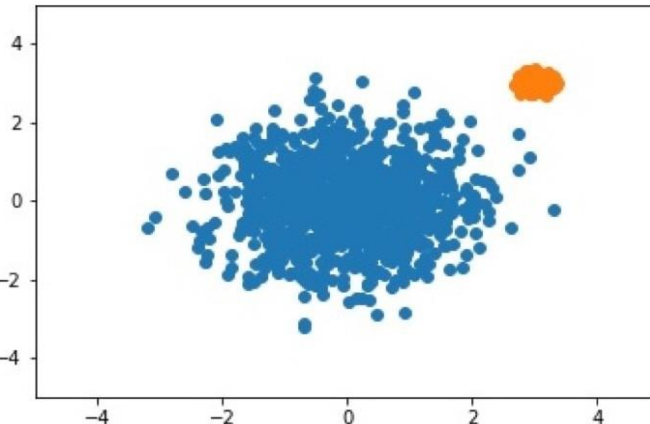
The constraints on $\Lambda_{\tilde{B}W}$ from unitarity bounds.

\sqrt{s} (GeV)	250	500	1000	3000	5000
$\Lambda_{\tilde{B}W}$ (GeV)	> 49.4	> 85.4	> 144.5	> 330.0	> 484.2

Constraint on coefficient of operator

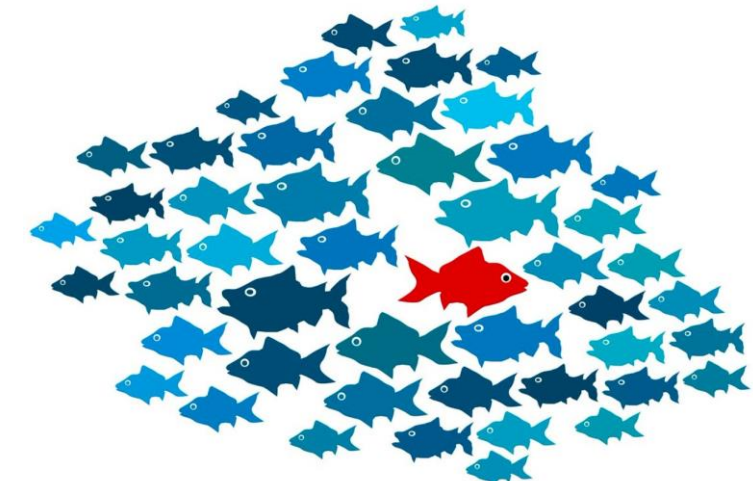
The unitarity bounds tell us the minimum integrated luminosity required to study nTGC and aQGC

Machine Learning: Anomaly detection

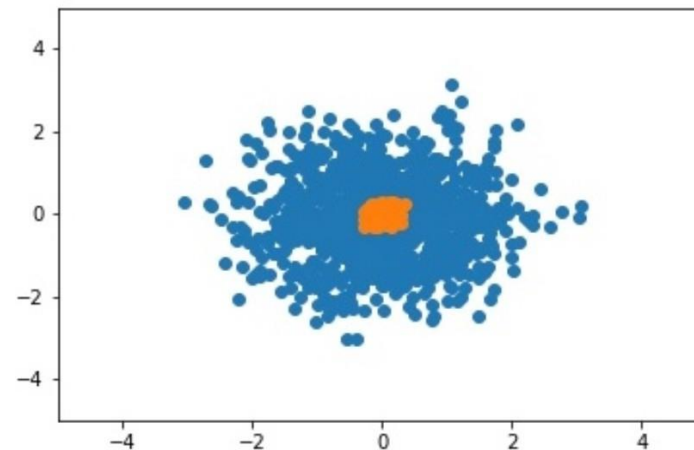


Outlier Detection

- Searching for unique or unexpected events
- In HEP, this is the tails of distributions or uncovered phase space

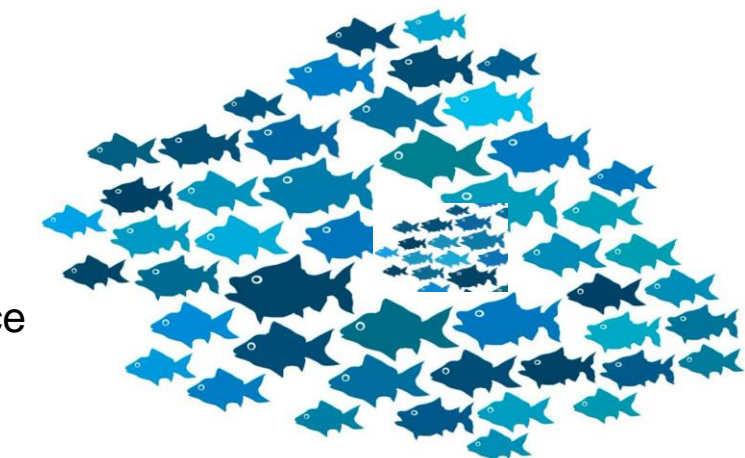


[1807.10261, 1808.08979, 1808.08992, 1811.10276, 1903.02032, 1912.10625, 2004.09360, 2006.05432, 2007.01850, 2007.15830, 2010.07940, 2102.08390, 2104.09051, 2105.07988, 2105.10427, 2105.09274, 2106.10164, 2108.03986, 2109.10919, 2110.06948, 2112.04958, 2203.01343, 2206.14225, 2303.14134, 2304.03836, 2306.03637, 2308.02671, 2309.10157, 2309.13111, ...]



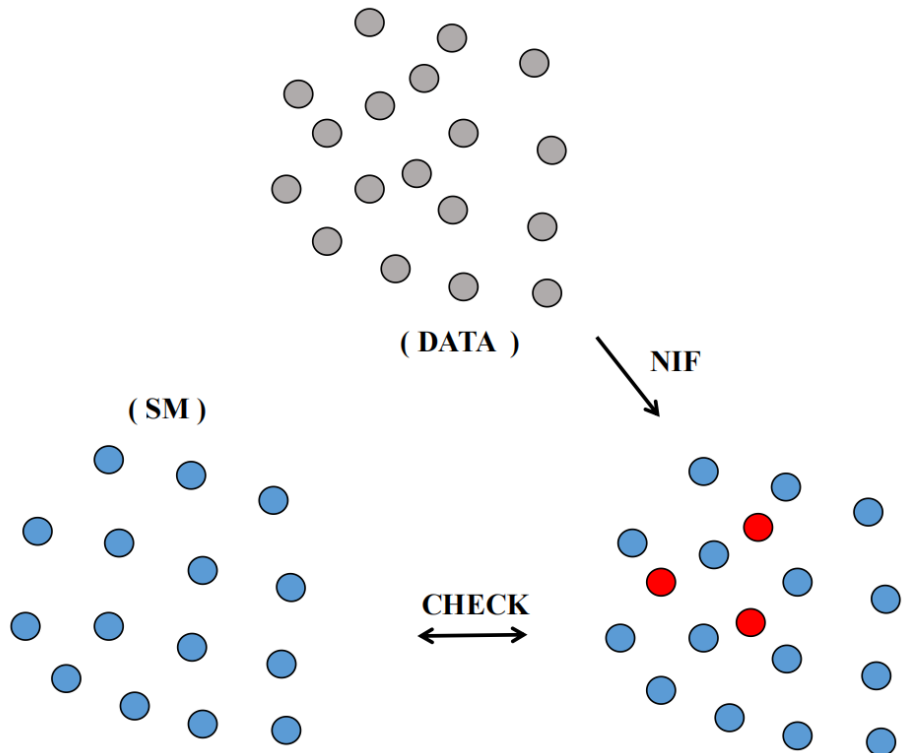
Overdensity detection

- Analogous to the traditional bump hunting
- Searching for new physics effect of interference term dominate



[1805.02664, 1806.02350, 1902.02634, 1912.12155, 2001.05001, 2001.04990, 2012.11638, 2106.10164, 2109.00546, 2202.00686, 2203.09470, 2208.05484, 2210.14924, 2212.11285, 2305.04646, 2305.15179, 2306.03933, 2307.11157, 2309.12918, 2310.06897, 2310.13057,]

Nested IF (NIF)

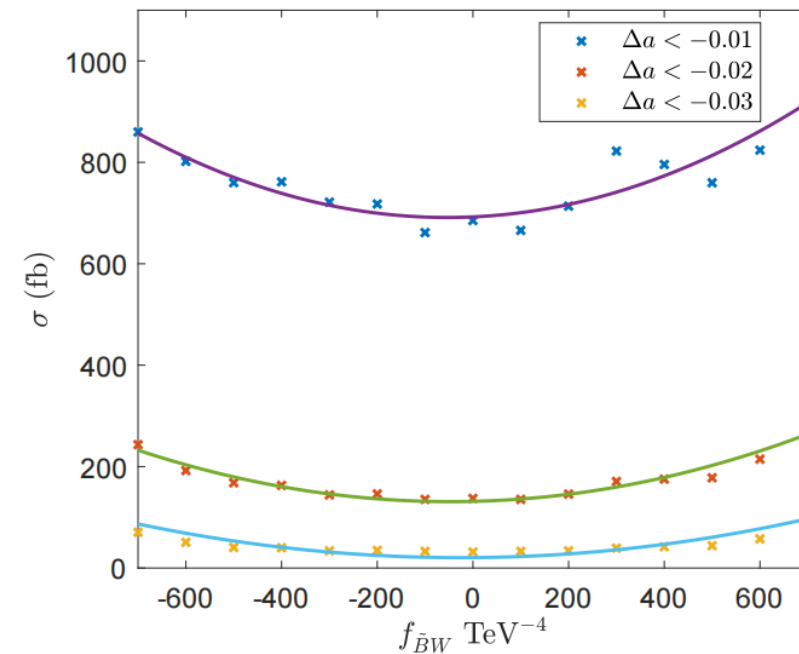
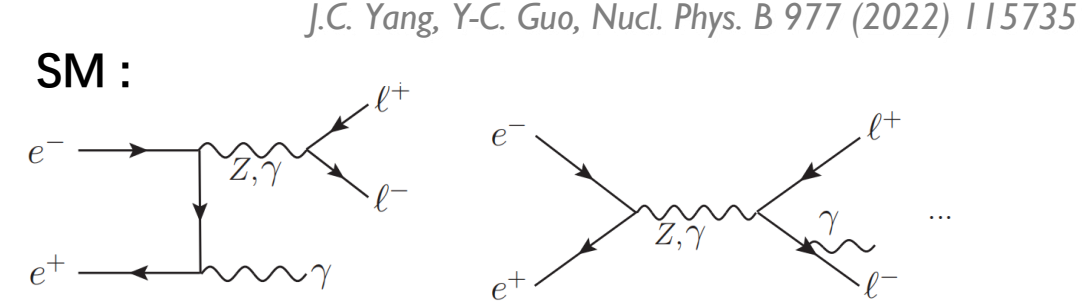
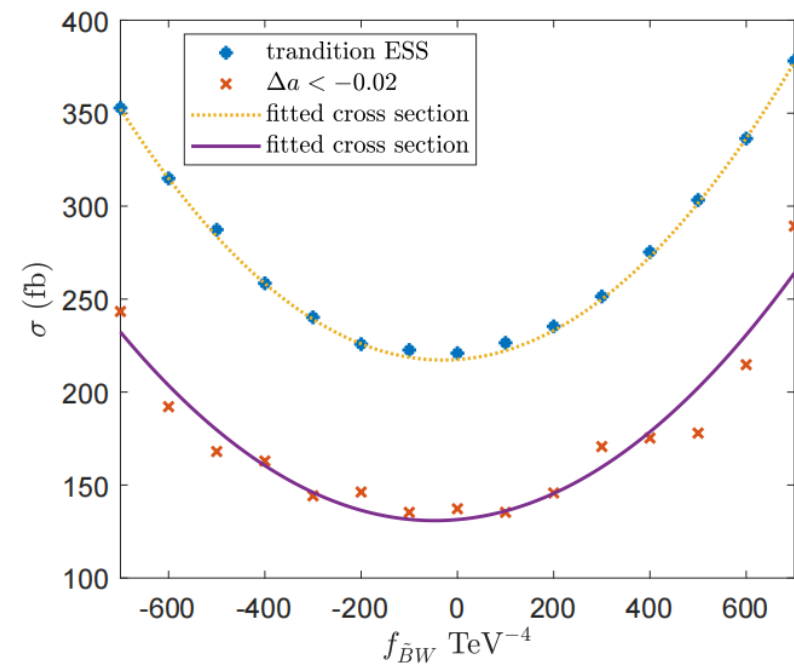
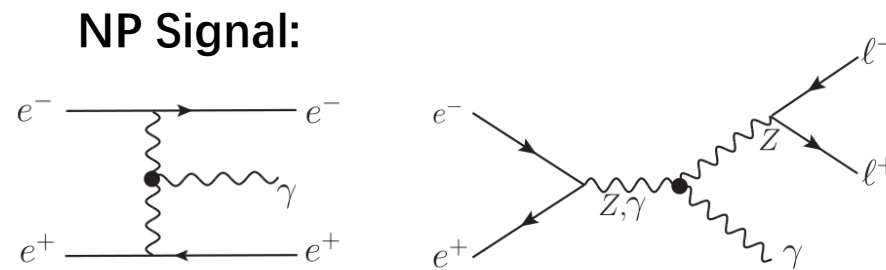


Nested Isolation Forest (NIF) :

- ✓ Interference effects dominate
- ✓ Training data set: SM data is used to establish the reference value of anomaly distribution
- ✓ Calculate the change in the anomaly score:
$$\Delta a^i = a_{data}^i - a_{SM}^i$$

NIF can identify the signals that overlap with the background through the distribution density

Search for nTGC by NIF in $e^+ e^- \rightarrow Z\gamma$

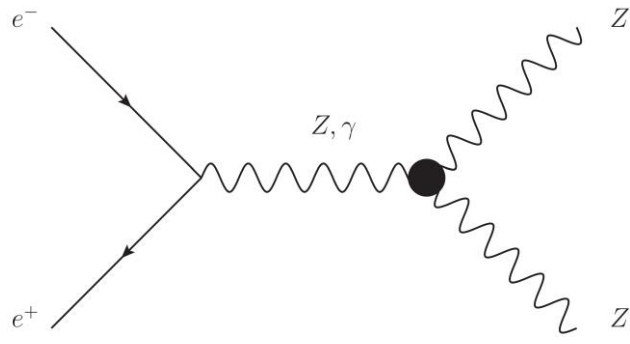


Left: Cross section obtained by kinematic analysis and NIF algorithm (function of f_{BW})
 Right: The effect of NIF algorithm with different conditions

Diboson productions (ZZ)

- nTGC in the $e^+ e^- \rightarrow ZZ$ process

Y.-C. Guo, C.J.Pan, M.Q.Ruan & J.C.Yang, to be uploaded to arXiv.org

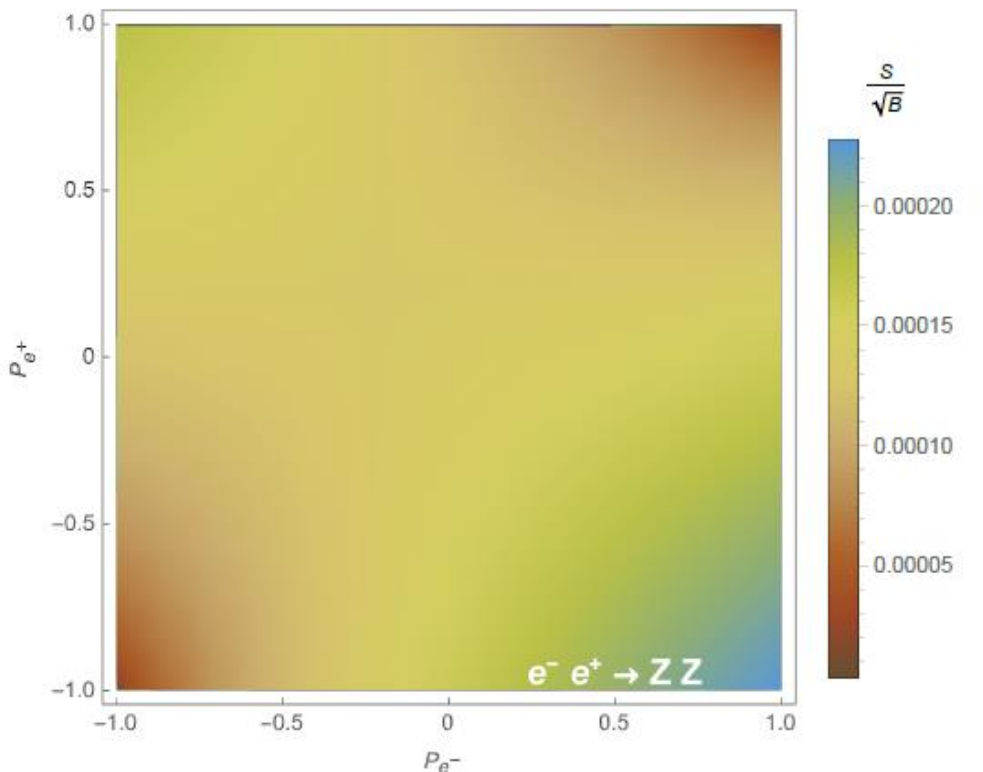


$$\sigma_{\text{pol}}^{\text{SM}}(ZZ) = - \left(16 (c_W^2 - 1)^2 (P_{e^+} + 1)(P_{e^-} - 1)s_W^4 + (1 - 2c_W^2)^4 (P_{e^+} - 1)(P_{e^-} + 1) \right) \\ \times \frac{e^4 \sqrt{s - 4M_Z^2} \left(\sqrt{s}(s - 2M_Z^2) \sqrt{4M_Z^2 - s} + (4M_Z^4 + s^2) \cot^{-1} \left(\frac{2M_Z^2 - s}{\sqrt{s}\sqrt{4M_Z^2 - s}} \right) \right)}{128\pi c_W^4 s^2 s_W^4 (2M_Z^2 - s) \sqrt{4M_Z^2 - s}},$$

$$\sigma_{\text{pol}}^{\text{int}}(ZZ) = \left(4 (c_W^2 - 1) (P_{e^+} + 1)(P_{e^-} - 1)s_W^2 + (1 - 2c_W^2)^2 (P_{e^+} - 1)(P_{e^-} + 1) \right) \\ \times \frac{e^2 M_Z^2 \sqrt{s - 4M_Z^2} \left(\sqrt{s}(2M_Z^2 + s) \sqrt{4M_Z^2 - s} + 4M_Z^2 (s - M_Z^2) \cot^{-1} \left(\frac{2M_Z^2 - s}{\sqrt{s}\sqrt{4M_Z^2 - s}} \right) \right)}{32\pi \Lambda_{BW}^4 c_W s^2 s_W \sqrt{4M_Z^2 - s}},$$

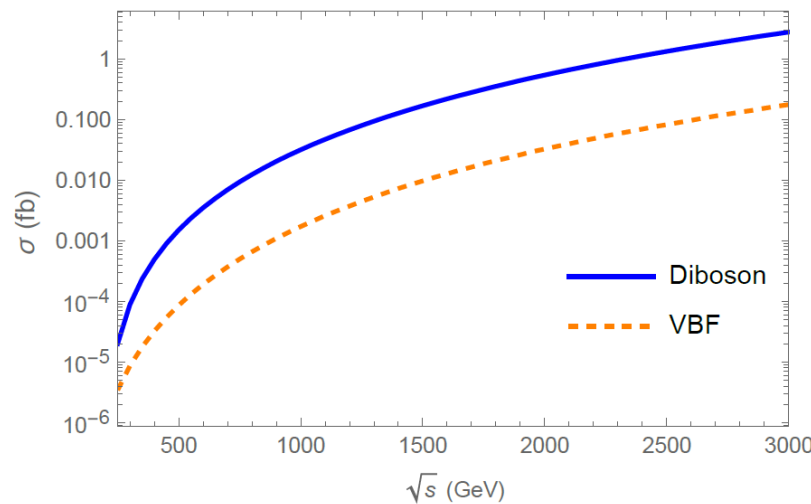
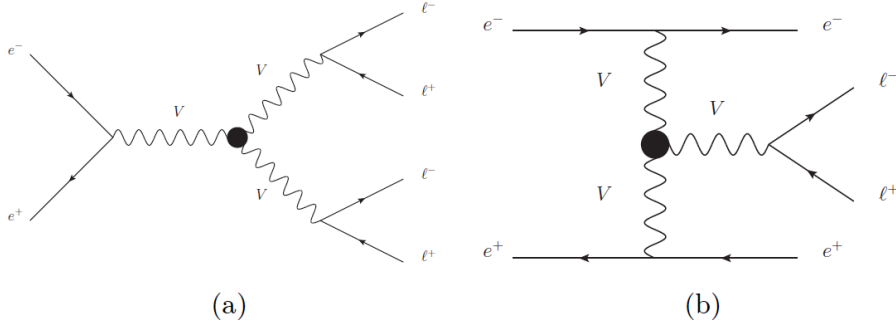
$$\sigma_{\text{pol}}^{\text{nTGC}}(ZZ) = - \frac{c_W^2 M_Z^2 s_W^2 (s - 4M_Z^2)^{\frac{5}{2}} (P_e - P_{e^+} - 1)}{24\pi \Lambda_{BW}^8 \sqrt{s}}.$$

Effect of initial beam polarization at e+e- Colliders

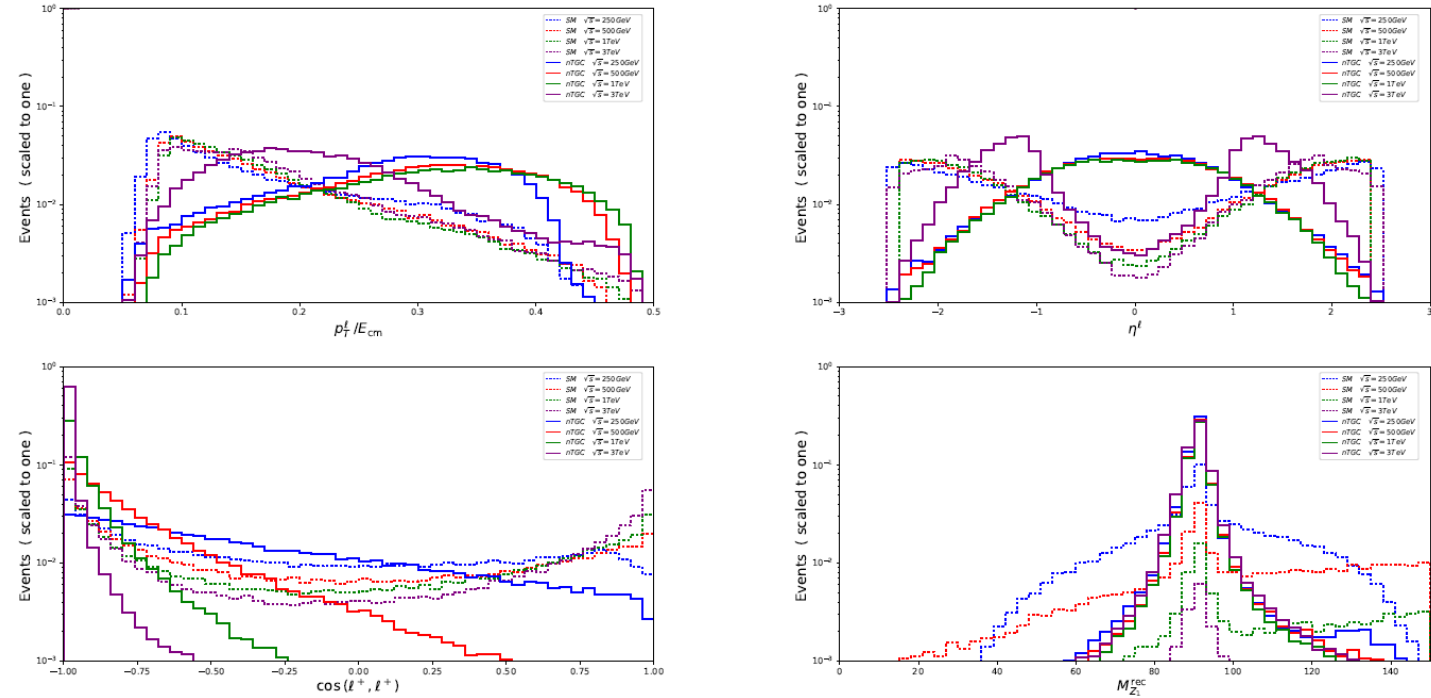


Diboson productions (ZZ)

- nTGC signal of $e^+e^- \rightarrow 2l\ 2l'$



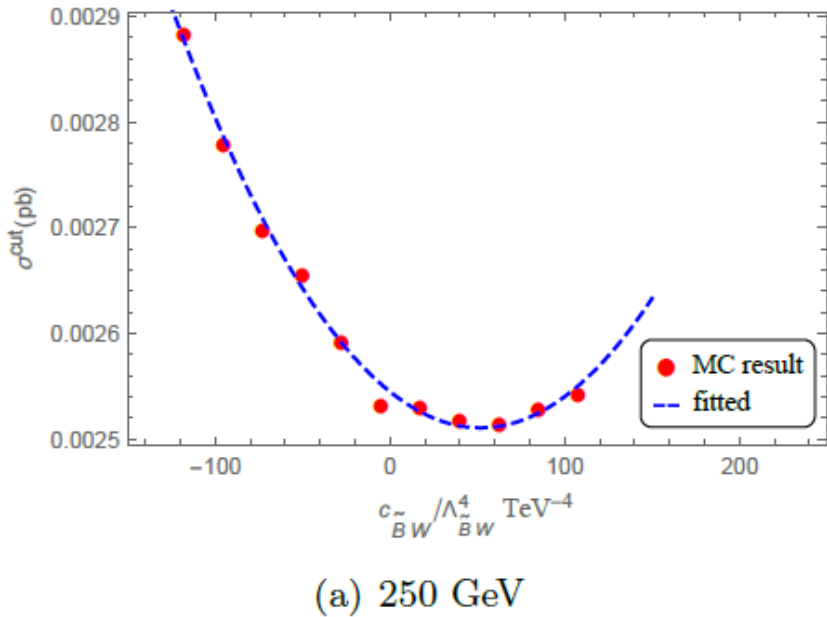
The normalized distributions of observables for ZZ leptonic decays



	$\sqrt{s}=250\text{ GeV}$		$\sqrt{s}=500\text{ GeV}$		$\sqrt{s}=1000\text{ GeV}$		$\sqrt{s}=3000\text{ GeV}$	
	SM	NP	SM	NP	SM	NP	SM	NP
Basic Cuts	22.83	0.254	11.64	0.161	5.301	0.109	1.336	0.022
$p_T^l/E_{\text{cm}} > 0.15$	11.01	0.228	5.696	0.148	2.625	0.101		
$ \eta^l < 1.5$	9.244	0.225	4.105	0.143	1.677	0.098		
$\cos(\ell^+, \ell^+) < 0.6$							0.567	0.022
$M_{Z_1, Z_2}^{\text{rec}} \in (80, 100) \text{ GeV}$	3.626	0.180	0.621	0.126	0.110	0.086	0.016	0.018
Efficiency ϵ	10%	46%	3.1%	49%	1.2%	47%	0.7%	60%

Diboson productions (ZZ)

$$\sigma_{\text{nTGC}}^{\text{ac}} = \epsilon_{\text{SM}} \sigma_{\text{SM}} + \epsilon_{\text{NP}} \sigma_{\text{NP}} + \frac{\text{sign}(c_{\tilde{B}W})}{\Lambda_{\tilde{B}W}^4} \hat{\sigma}_{\text{int}},$$



$$S_{\text{stat}} = \sqrt{2[(N_{\text{bg}} + N_s) \ln(1 + N_s/N_{\text{bg}}) - N_s]}$$

Table 5: The expected constraints on $\text{sign}(c_{\tilde{B}W})/\Lambda_{\tilde{B}W}^4$ (TeV $^{-4}$) for $e^+e^- \rightarrow 2\ell 2\ell'$ at each energy point of CEPC, ILC and CLIC with corresponding design luminosities.

S_{stat}	\sqrt{s} (GeV)			
	250	500	1000	3000
2	[-10.2, 96.2]	[-5.5, 13.3]	[-0.84, 1.26]	[-0.066, 0.074]
3	[-14.7, 100.7]	[-7.4, 15.3]	[-1.10, 1.52]	[-0.084, 0.092]
5	[-22.8, 108.7]	[-10.9, 18.6]	[-1.56, 1.98]	[-0.115, 0.123]

- $ee \rightarrow ZZ \rightarrow 2l 2l'$
- $ee \rightarrow ZZ \rightarrow 4j$
- $ee \rightarrow ZZ \rightarrow lljj$
- $ee \rightarrow ZZ \rightarrow ll\nu\bar{\nu}$
- $ee \rightarrow ZZ \rightarrow jj\nu\bar{\nu}$

Combine on the Coefficients for different Channels of Z Decays

S_{stat}	\sqrt{s} (GeV)			
	250	500	1000	3000
2	[-4.1, 4.7]	[-0.58, 0.59]	[-0.12, 0.20]	[-0.0032, 0.0036]
3	[-6.0, 7.2]	[-0.80, 0.81]	[-0.16, 0.25]	[-0.0040, 0.0044]
5	[-9.2, 11.2]	[-1.15, 1.17]	[-0.22, 0.32]	[-0.0054, 0.0058]

Summary

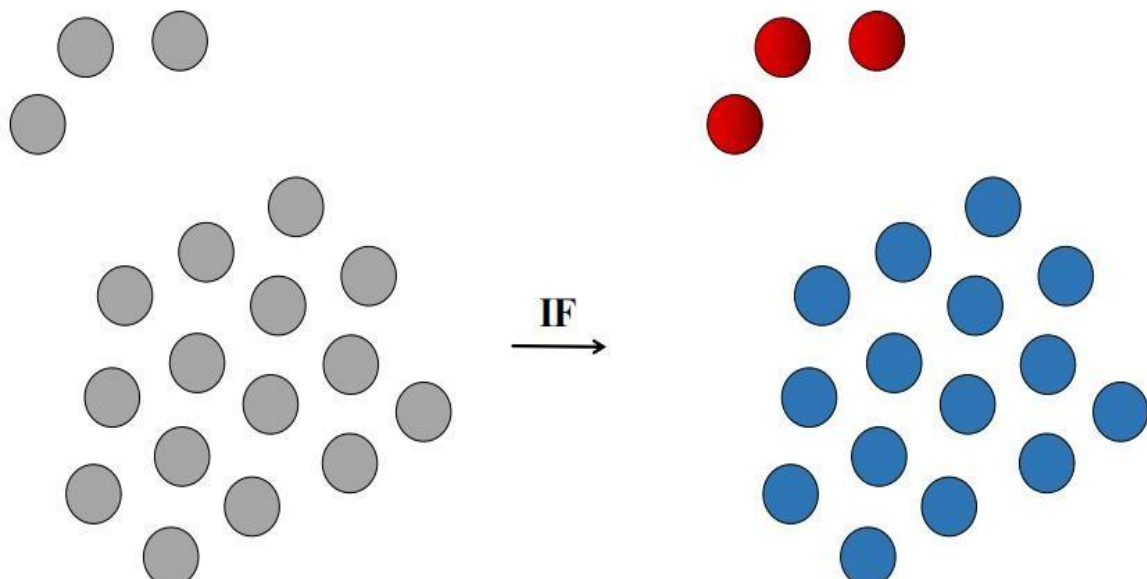
- ALP appears naturally in broad extensions of the SM. The CEPC can complement LHC measurements of ALP coupling to SM particles.
- Search for new physics indirectly as well as directly. nTGCs provide windows of opportunity for probing indirectly possible physics BSM
- Polarized beams optimize measurement of coupling to axion-like particles, as well as nTGCs.
- Testing entanglement and Bell inequalities in di-boson production can bring new opportunities to CEPC

Thank you !



Back up

Isolation Forest (IF)

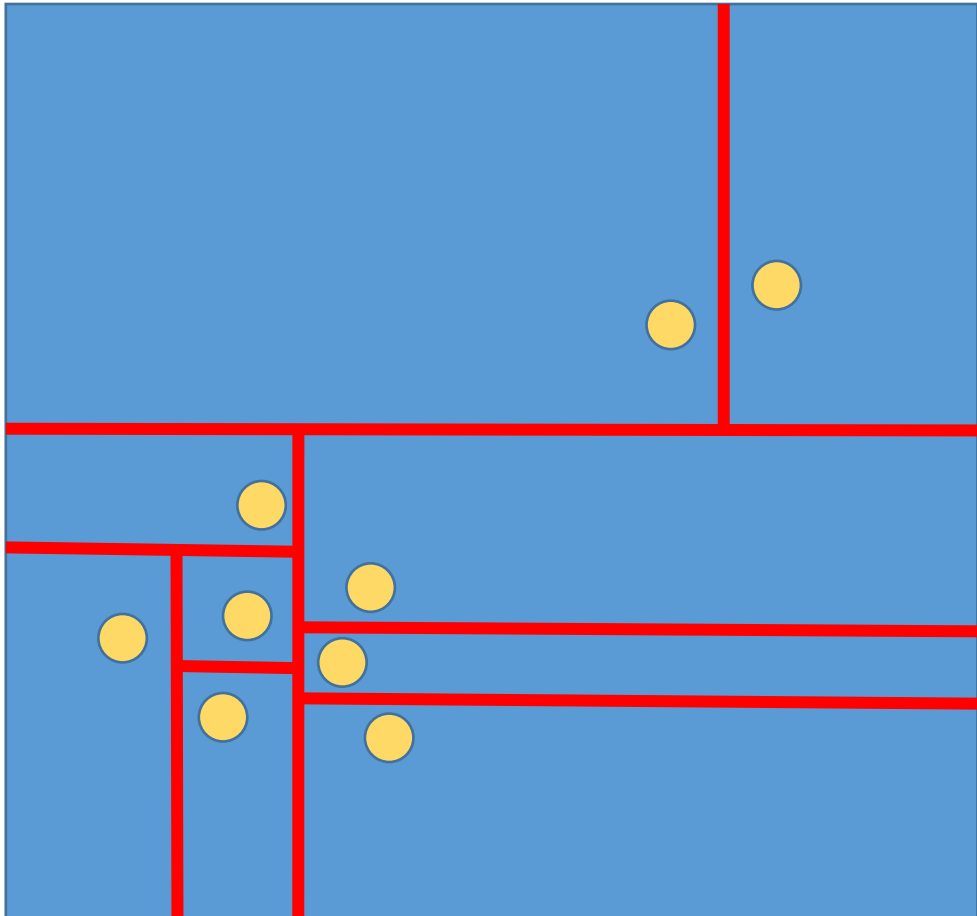


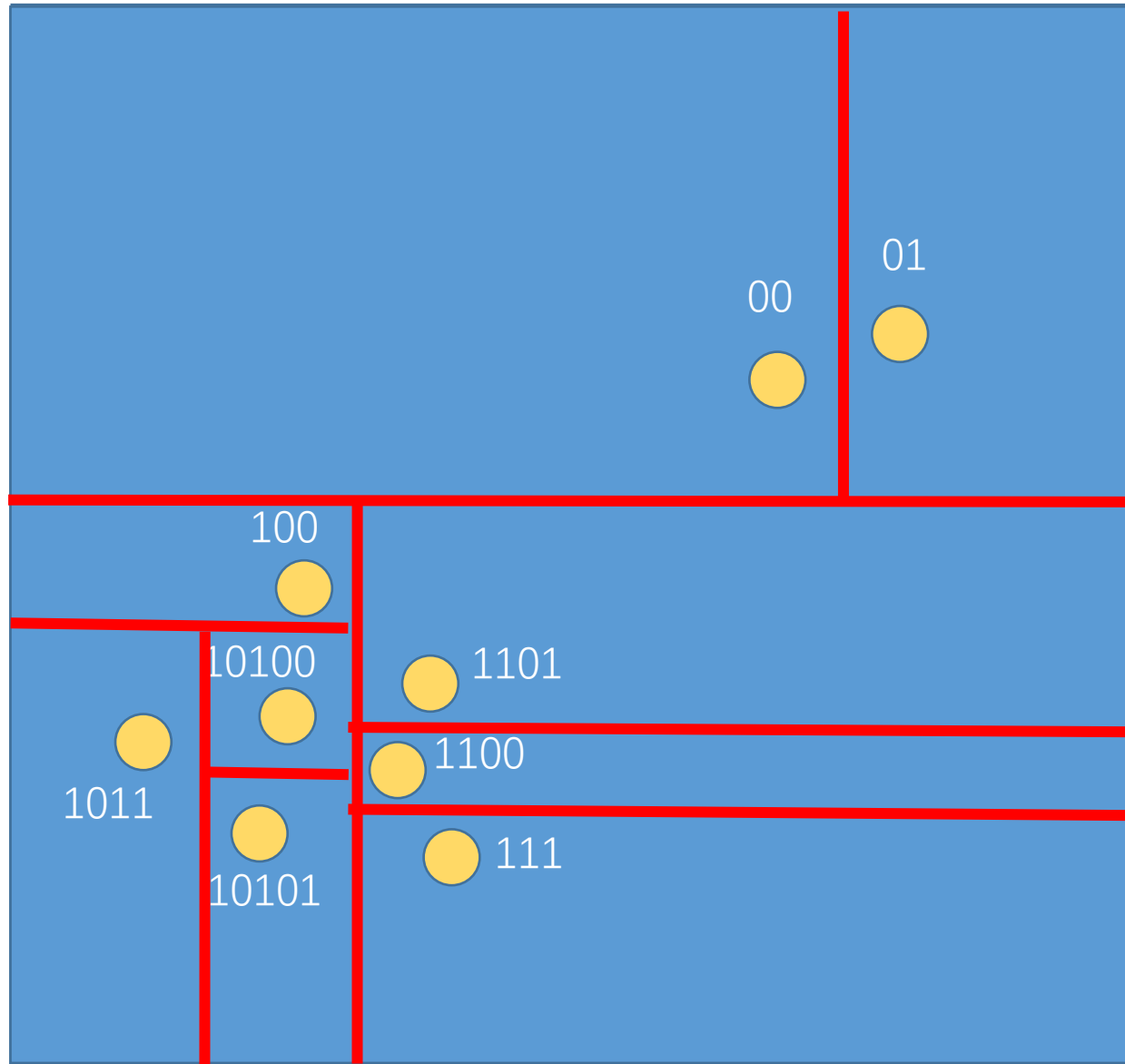
- IF : “**Few and different**” anomaly event
New physics signal
- Anomaly score a : quantify the distance of the data point from the center point of all events

F. T. Liu, K. M. Ting and Z. Zhou, *Isolation forest*, in 2008 Eighth IEEE International Conference on Data Mining, pp. 413–422, 2008, [DOI](#).

Isolation tree

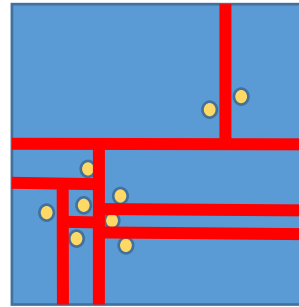
- Randomly choose a undivided leaf
- Randomly choose a dimension
- Divide
- Repeat until every node is either partitioned.



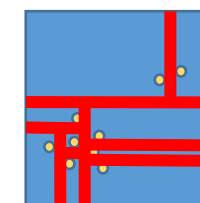
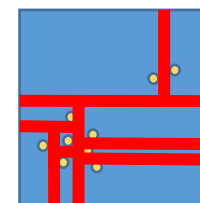
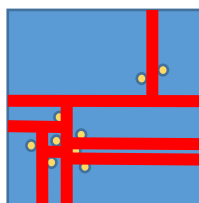
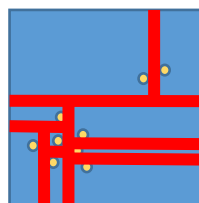
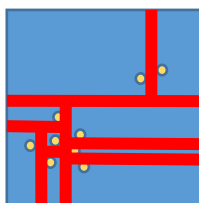
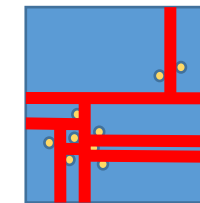
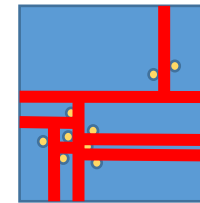
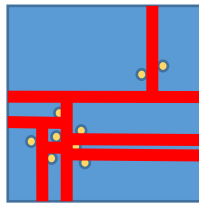
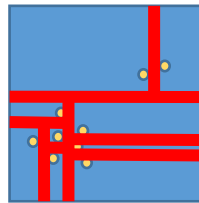
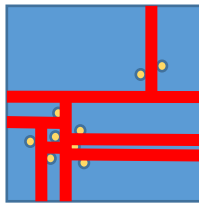


Tree -> Forest

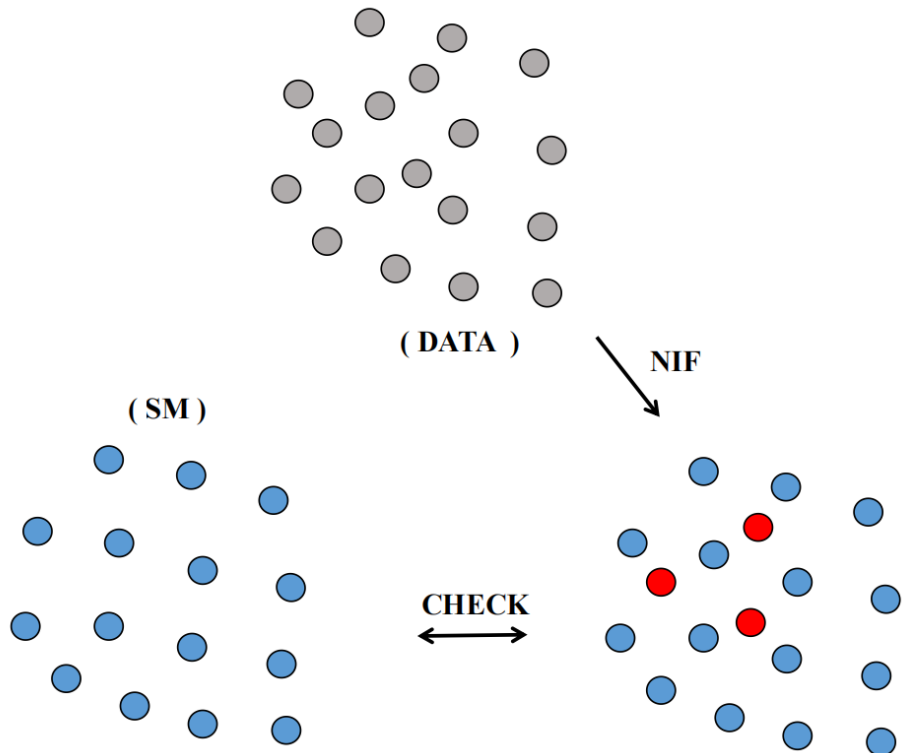
- Isolation tree:



- Isolation forest:



Nested IF (NIF)



Nested Isolation Forest (NIF) :

- ✓ **Interference** effects dominate
- ✓ Training data set: SM data is used to establish the reference value of anomaly distribution
- ✓ Calculate the change in the anomaly score:
$$\Delta a^i = a_{data}^i - a_{SM}^i$$

NIF can identify the signals that overlap with the background through the distribution density